



**Neo-Tethys geodynamics and mantle convection: from extension to compression in Africa and a conceptual model for obduction**

Journal:	<i>Canadian Journal of Earth Sciences</i>
Manuscript ID	cjes-2015-0118.R1
Manuscript Type:	Article
Date Submitted by the Author:	07-Dec-2015
Complete List of Authors:	Jolivet, Laurent; Université d'Orléans, ISTO Faccenna, Claudio; Università Roma Tre, Dipartimento di Scienze Agard, Philippe; Université Pierre et Marie Curie, Institut des Sciences de la Terre Paris Frizon de Lamotte, Dominique; Université de Cergy Pontoise, Département des Sciences de la Terre et de l'Environnement Menant, Armel; Université d'Orléans, ISTO Sternai, Pietro; California Institute of Technology, Guillocheau, François; Université de Rennes 1, Géosciences Rennes
Keyword:	Convection, Obduction, reconstructions, geodynamics, tectonics

SCHOLARONE™  
 Manuscripts

1 **Neo-Tethys geodynamics and mantle convection: from extension to compression in**  
2 **Africa and a conceptual model for obduction**

3  
4 Laurent Jolivet <sup>(1,2,3)</sup>, Claudio Faccenna <sup>(4)</sup>, Philippe Agard <sup>(5)</sup>, Dominique Frizon de Lamotte  
5 <sup>(6)</sup>, Armel Menant <sup>(1,2,3)</sup>, Pietro Sternai <sup>(7)</sup> and François Guillocheau <sup>(8)</sup>

6  
7 (1) Univ d'Orléans, ISTO, UMR 7327, 45071 Orléans, France ([laurent.jolivet@univ-orleans.fr](mailto:laurent.jolivet@univ-orleans.fr))

8 (2) CNRS/INSU, ISTO, UMR 7327, 45071 Orléans, France

9 (3) BRGM, ISTO, UMR 7327, BP 36009, 45060 Orléans, France

10 (4) Laboratory of Experimental Tectonics, Dipartimento di Scienze, Università Roma TRE, Largo  
11 S.L.Murialdo 1 - 00143 Roma, Italy ([faccenna@uniroma3.it](mailto:faccenna@uniroma3.it))

12 (5) Sorbonne Universités, UPMC Univ Paris 06, UMR 7193 CNRS-UPMC, Institut des Sciences de la  
13 Terre Paris (ISTeP), F-75005 Paris, France ([philippe.agard@upmc.fr](mailto:philippe.agard@upmc.fr))

14 (6) Université de Cergy-Pontoise, Département géosciences et environnement. 95300 □Cergy-Pontoise,  
15 France ([Dominique.Frizon-De-Lamotte@u-cergy.fr](mailto:Dominique.Frizon-De-Lamotte@u-cergy.fr))

16 (7) Department of Earth Sciences, □University of Cambridge □Bullard Laboratories, Madingley  
17 road □Cambridge, Cambridgeshire CB3 0EZ, United Kingdom ([psternai@caltech.edu](mailto:psternai@caltech.edu))

18 (8) Géosciences Rennes, UMR 6118 CNRS, Université de Rennes 1, Campus de Beaulieu, 35042 Rennes  
19 Cedex, France ([francois.guillocheau@univ-rennes1.fr](mailto:francois.guillocheau@univ-rennes1.fr))

20  
21 **Abstract:** Since the Mesozoic, Africa has been under extension with shorter periods of  
22 compression associated with obduction of ophiolites on its northern margin. Less frequent  
23 than “normal” subduction, obduction is a first order process that remains enigmatic. The  
24 closure of the Neo-Tethys Ocean, by the Upper Cretaceous, is characterized by a major  
25 obduction event, from the Mediterranean region to the Himalayas, best represented around the  
26 Arabian Plate, from Cyprus to Oman. These ophiolites were all emplaced in a short time  
27 window in the Late Cretaceous, from ~100 to 75 Ma, on the northern margin of Africa, in a  
28 context of compression over large parts of Africa and Europe, across the convergence zone.  
29 The scale of this process requires an explanation at the scale of several thousands of  
30 kilometres along strike, thus probably involving a large part of the convecting mantle. We  
31 suggest that alternating extension and compression in Africa could be explained by switching  
32 convection regimes. The extensional situation would correspond to steady-state whole-mantle  
33 convection, Africa being carried northward by a large-scale conveyor belt, while compression  
34 and obduction would occur when the African slab penetrates the upper-lower mantle  
35 transition zone and the African plate accelerates due to increasing plume activity, until full  
36 penetration of the Tethys slab in the lower mantle across the 660 km transition zone during a  
37 25 Myrs-long period. The long-term geological archives on which such scenarios are founded  
38 can provide independent time constraints for testing numerical models of mantle convection  
39 and slab/plume interactions.

40  
41

42 **Résumé:** Depuis le Mésozoïque, l'Afrique a été en extension avec de courtes périodes de  
43 compression associées à l'obduction d'ophiolites sur sa marge nord. Moins fréquente que la  
44 subduction, l'obduction est néanmoins un phénomène de premier ordre qui reste énigmatique.  
45 La fermeture de la Neo-Téthys au Crétacé supérieur est caractérisée par un épisode majeur  
46 d'obduction, depuis la Méditerranée jusqu'à l'Himalaya, en particulier sur la marge de  
47 l'Arabie, de Chypre à l'Oman. Ces ophiolites furent toutes mises en place dans un court laps  
48 de temps pendant le Crétacé supérieur, de 100 à 75 Ma, dans un contexte de compression  
49 enregistré en de larges portions de l'Afrique et de l'Europe, au travers de la zone de  
50 convergence. L'échelle de ce processus requiert une explication à l'échelle de plusieurs  
51 milliers de kilomètres et donc impliquant vraisemblablement l'ensemble du manteau  
52 convectif. Nous suggérons que l'alternance de périodes extensives et compressives en Afrique  
53 résulte de changements du régime convectif. Les périodes extensives correspondraient à la  
54 convection impliquant tout le manteau, l'Afrique étant portée par une grande cellule de type  
55 tapis-roulant, tandis que la compression et l'obduction se produiraient quand le panneau  
56 plongeant africain pénètre la transition entre le manteau supérieur et le manteau inférieur et  
57 quand la plaque Afrique accélère en conséquence d'une plus grande activité du panache,  
58 jusqu'à pénétration complète, durant une période d'environ 25 Ma. Les archives géologiques  
59 sur lesquelles ce type de scénarios est fondé peuvent fournir des contraintes temporelles  
60 indépendantes pour tester les modèles numériques de convection mantellique et les  
61 interactions panache/panneau plongeant.

62

63 **Keywords :** convection, obduction, reconstructions, geodynamics, tectonics

64

65

66           **Introduction:** One of the characteristics of mountains formed during closure of the  
67 Neo-Tethys Ocean is the existence of large ophiolitic nappes, remnants of oceanic lithosphere  
68 (Gass 1968; Coleman 1977; 1981; Dewey 1976). Some of these ophiolites were deeply  
69 subducted, metamorphosed and exhumed to the surface like most of Alpine ones (Oberhänsli  
70 et al. 2004; Lardeaux et al. 2006; Angiboust et al. 2009), whereas others were simply thrust  
71 over the continental margin, despite an *a priori* higher density, escaping metamorphism (like  
72 the Semail ophiolite in Oman or the Lycian ophiolite in Turkey (Coleman 1981; Okay 1989;  
73 Ricou 1971; Sengör and Yilmaz 1981) or again the Newfoundland ophiolites (Kidd et al.  
74 1978; Dewey and Casey 2013), through a process called obduction. One of the best-  
75 documented examples is the Late Cretaceous obduction of the Tethys ocean floor. Two  
76 episodes of obduction of oceanic nappes on the northern continental margin of Apulia and  
77 Africa are recognized, one in the Late Jurassic-Early Cretaceous in the Dinarides (Dercourt et  
78 al. 1986; Schmid et al. 2008) and one in the Late Cretaceous, from Greece to Oman (Ricou  
79 1971; Coleman 1981; Okay and Tüysüz 1989) for which Sengör and Stock (2014) recently  
80 coined the name Ayyubid Orogen.

81           The Neo-Tethys realm is characterized by a second feature: the Apulian (or Adria)  
82 microcontinent was separated from Africa sometime in the Jurassic (Ricou 1994; Barrier and  
83 Vrielynck 2008; Frizon de Lamotte et al. 2011; Ricou 1994) and drifted away to collide with  
84 Eurasia, forming the Mediterranean belts from the Late Cretaceous onward. At a later stage,  
85 Arabia was detached from Africa from the Late Eocene (Jolivet and Faccenna 2000;  
86 Bellahsen et al. 2003; McQuarrie et al. 2003). This process of rifting of continental blocks  
87 away from the northern margin of Africa also occurred much earlier in the Permian when the  
88 Cimmerian blocks rifted away from Africa (Matte 2001) or even earlier in the Devonian when  
89 the Paleotethys Ocean formed at the expense of the Rheic Ocean (Stampfli and Borel 2002).  
90 Earlier, identical processes were active several times along the Palaeozoic when Avalonia,  
91 Armorica and Hun terranes rifted away from Gondwana (Matte 2001; Stampfli and Borel  
92 2002). We are thus searching for a conceptual model that could explain these two main  
93 features, (1) obduction and (2) fragmentation of the northern part of the southern continent  
94 and northward travel of the rifted blocks, at the scale of several thousands of kilometres. We  
95 herein present a model based on an extensive compilation of geological observations on the  
96 obduction process itself and on the large-scale geological evolution of Africa and surrounding  
97 mid-ocean ridges.

98

## 99           **1. Obduction of the Neo-Tethys ophiolites**

100

101 High-pressure and low-temperature (HP-LT) metamorphic conditions recorded in the  
102 tectonic units found below ophiolites do not differ from those retrieved in Alpine-type  
103 mountain belts and show that obduction results from subduction of the former continental  
104 margin below the oceanic lithosphere (Goffé et al. 1988; Searle et al. 1994; 2004; Yamato et  
105 al. 2007). Small units made of metamorphic units of oceanic origin, the so-called  
106 metamorphic sole, sandwiched between the ophiolite and the subducted margin, sign the first  
107 stages of obduction. These are characterized instead by high-temperature and low-pressure  
108 (HT-LP) metamorphic conditions and are systematically older than the HP-LT metamorphic  
109 rocks of the subducted continental margin (Hacker 1991; Hacker et al. 1996; Agard et al.  
110 2007).

111 In Oman or Western Turkey, the radiometric ages of magmatic rocks from the obducted  
112 ophiolite or the biostratigraphic ages of supra-ophiolite pelagic sediments, such as  
113 radiolarites, show that the ophiolite was very young ( $< \sim 5$  Myrs) at the time of obduction  
114 (Nicolas 1989; Rioux et al. 2013; Celik et al. 2006) implying the formation of an oceanic  
115 basin along the southern Neo-Tethys margin a few Myrs before obduction. Two types of  
116 models are debated for the Late Cretaceous obduction (Rioux et al. 2013): either subduction  
117 initiation along or near a mid-ocean ridge (Nicolas 1989) or formation of intra-oceanic  
118 subduction and later oceanic accretion in the upper plate as a result of mantle upwelling  
119 (Pearce et al. 1981; Rioux et al. 2013; MacLeod et al. 2013). Whether this young basin was  
120 formed as a back-arc basin above a north-dipping subduction, as a prelude to obduction, or  
121 along a new mid-ocean ridge is beyond the scope of this paper, but the two models have  
122 drastically different consequences. In the latter case, this new subduction would result from  
123 the same compressional episode as obduction, but there is then only a short time from the  
124 formation of the first intra-oceanic thrust, the formation of a back-arc basin to its obduction.  
125 In the former case, the cause for the formation of this new ridge remains enigmatic but it  
126 could be part of the generalized extension that predates compression. In this particular case  
127 the age of the ophiolite should be older than the beginning of compression (i.e. provided by  
128 metamorphic sole ages). By contrast, the ophiolite in Armenia was much older at the time of  
129 obduction and published models suggest the existence of an intra-oceanic subduction and a  
130 long-lived intra-oceanic back-arc domain where the ophiolite would have been rejuvenated  
131 before it was obducted (Rolland et al. 2009; Hässig et al. 2013; 2015a; 2015b).

132 These different models, obduction starting at the mid-oceanic ridge or as an intra-  
133 oceanic subduction associated with back-arc extension (supra-subduction zone ophiolites),

134 provide good explanations for the evolution of metamorphic rocks found below the ophiolites,  
135 the high-temperature and low-pressure (HT-LP) sole or the HP-LT blueschists and eclogites  
136 in the subducted margin (Searle et al. 2004; Yamato et al. 2007), but not for the subduction  
137 initiation precluding to obduction.

138 What is then the cause of the initial thrusting leading to obduction? This question has  
139 been approached by two different models: (i) acceleration of convergence, as a result of  
140 regional-scale plate reorganization (Agard et al. 2006), that makes subduction more difficult  
141 below Eurasia and induces transmission of compression within the subducting plate that  
142 buckles and finally breaks (Agard et al. 2007), or (ii) enhanced compression by increasing  
143 mantle plume activity (Vaughan and Scarrow 2003). Open questions include the cause of  
144 plate acceleration inducing compression and the cause for the asymmetry of the resulting  
145 subduction, always northward (i.e. south-directed obduction) in the case of the Neo-Tethys.

146

## 147 **2. Tectonic history of Africa and the Neo-Tethys Ocean**

148

149 A series of reconstructions (Fig. 1) and a compilation of geological events (Fig. 2) show  
150 the succession of events in the Neo-Tethys Ocean and Africa since the Jurassic. In the Middle  
151 Jurassic (~170 Ma, figure 1A), the Neo-Tethys, widely opened in the east, subducts below the  
152 southern margin of Eurasia (Agard et al. 2011 and references therein), making its connection  
153 with the Atlantic through the Alpine Tethys (Dercourt et al. 1986; Ricou 1994). In the  
154 meantime, a second-order rifted basin develops within Africa (Frizon de Lamotte et al. 2011)  
155 and the rifted Apulian s.l. continent migrates northward with respect to Africa, forming the  
156 Eastern Mediterranean basin (Ricou 1994). The Western Indian Ocean starts to open by  
157 rifting between India and Africa during the same period (see a recent review in Frizon de  
158 Lamotte et al. 2015). At the end of the Jurassic, the Dinaric ophiolites are emplaced on the  
159 northern margin of the Apulian block, as a result of the onset of intra-oceanic subduction  
160 dated by metamorphic soles at 175-160 Ma (Agard et al. 2007).

161 In the Early Cretaceous (~120 Ma, figure 1B), the African Plate is entirely under  
162 tension and numerous rifts develop within Africa and Arabia (Guiraud et al. 2005, Frizon de  
163 Lamotte et al. 2015), while the South Atlantic Ocean opens. Back-arc basins develop above  
164 the northern subduction zone, forming oceanic crust now flooring the Black Sea and the  
165 Caspian Sea and small back-arc domains in Central Iran (Hippolyte et al. 2010; Nikishin et al.  
166 1998; 2015a; 2015b; Agard et al. 2011). Since the Jurassic, an intra-oceanic subduction

167 induces back-arc spreading, forming the ophiolite that will be obducted later on the northern  
168 margin of Apulia in Armenia (Hässig et al. 2013; 2015a; 2015b).

169         After a significant plate reorganization and increase of the Africa-Eurasia convergence  
170 velocity at ~118 Ma (Agard et al. 2007), continuing extension on the northern margin of  
171 Gondwana and on the active southern margin of Eurasia from 120 to 95 Ma, compression is  
172 recorded in Africa and Europe in the Late Cretaceous (Figures 1 C and 1D) (Bosworth et al.  
173 1999; Guiraud et al. 2005). It is preceded by a short event at about 110 Ma characterized by  
174 the reactivation of N-S trending structures (the so-called “Austrian” phase) mainly observed  
175 in Western Africa and independent from the Africa-Eurasia convergence. Except for this short  
176 earlier event, including the whole obduction process, the compressional episode lasted from  
177 ~100 to ~75 Ma. This first compressional event is coeval with the initiation of the intra-  
178 oceanic subduction leading to obduction and forming the large ophiolitic nappes observed  
179 nowadays (Figure 1C). The age of this initiation is best constrained by the ages of  
180 metamorphic soles that all cluster around 100-95 Ma. Compression then progressively  
181 propagates over a large part of Africa with basement undulations and compressional  
182 reactivation of the previously formed rifts at about 85 Ma, i.e. the so-called Santonian event  
183 (Benkhelil 1988; 1989; Genik 1993; Bosworth et al. 1999; Guiraud et al. 2005; Bevan and  
184 Moustafa 2012; Arsenikos et al. 2013) (Figure 1D). This Santonian event is not present  
185 everywhere but it is well characterized in the northern part of Africa and Arabia and also  
186 along the E-W segment of the Sub-Sahara Rift System. It has apparently not been recorded  
187 everywhere and some regions such as the Sirt basin or the Muglad Rift in Sudan have not  
188 been reactivated (McHargue et al. 1992; Wennekers et al. 1996) but it is nevertheless widely  
189 distributed all over the northern half of Africa.

190         A special attention should be paid to the Sirt basin. This basin developed from the  
191 Early Cretaceous to the Present on top of a highly pre-structured and faulted Panafrican  
192 basement with a Proterozoic metamorphic basement and a Paleozoic to Early Cenozoic cover  
193 (Wennekers et al. 1996; Abadi et al. 2008). Thick accumulations of sediments developed in  
194 the Cretaceous with the irregular deposition of the lower Cretaceous, followed by a period of  
195 major syn-rift subsidence during the Cenomanian and Turonian and then by the transgressive  
196 deposition of the Late Cretaceous up to the end of the Cretaceous. So, in Sirt, the Late  
197 Cretaceous contractional event is only underlined by a decrease of the subsidence rate (Frizon  
198 de Lamotte et al. 2011). An additional observation may explain why the Late Cretaceous  
199 inversion is not obvious in the Sirt Basin. The main depot-centres of the Sirt Basin strike NW-  
200 SE, almost perpendicular to the compressional fold axes in the nearby Cyrenaica (Arsenikos



201 et al. 2013). The development of these basins in the Jurassic and Cretaceous was highly  
202 influenced by the pre-existing faults and basins with that same strike (Wennekers et al. 1996).  
203 The compression recorded in Cyrenaica was not properly oriented to reactivate the Sirt Basin  
204 normal faults.

205 Compression is also recorded during the same period across Western Europe, from the  
206 Pyrenees where compression starts in the Santonian (~85 Ma, Vergès et al. 2002; Jammes et  
207 al. 2010) and south-eastern France, all the way to the Paris Basin and the North Sea  
208 (Guillocheau et al. 2000), ending up with slow subduction initiation in the western  
209 Mediterranean (the future Apennines subduction zone). During the same period, between 95  
210 and 85 Ma, blueschists forming in the subduction zone are exhumed to shallow depth along  
211 the southern margin of Eurasia along thousands of kilometres (Agard et al. 2006; 2007;  
212 Monié and Agard 2009).

213 After a period of relative quiescence between 65 and 45 Ma (Rosenbaum et al. 2002), the  
214 Middle-Late Eocene shows renewed compression (figure 1E) in the Atlas mountains,  
215 Cyrenaica, Syrian Arch and all the way to the Zagros (Arsenikos et al. 2013;  
216 Frizon de Lamotte et al. 2011) and north of the young west Mediterranean subduction zone in  
217 the Iberian Range and the Pyrenees (Vergès et al. 2002). This new compressional period  
218 preceded the Oligocene uplift of large parts of Africa (Burke et al. 2003; Burke and Gunnell,  
219 2008) amounting to 200-300 m in North Africa, coeval with the early formation of the North  
220 African volcanic province (Liégeois et al. 2005; Wilson 1993; Wilson and Guiraud 1992).  
221 Volcanism is recorded earlier in the Central Sahara, as early as 34 Ma (Ait-Hamou 2006). The  
222 uplift is for instance recorded during the Early Oligocene in the Niger Delta (Petters 1983)  
223 associated with a major regression but its exact age is poorly constrained. Otherwise, the  
224 upper plate of the convergence zone to the east records extensional deformation during this  
225 period.

226 A major change in subduction dynamics then occurs around 30-35 Ma (figure 1F), and  
227 back-arc basins start to form in the Mediterranean (Jolivet and Faccenna 2000). Meanwhile,  
228 rifting starts along the future Gulf of Aden and Red Sea, coeval with the Afar plume-related  
229 traps, and most of the sub-Saharan rifts are reactivated. The Miocene and Present stages  
230 (Figures 1G and 1H) are the continuation of the same situation with separation of Arabia from  
231 Africa, and opening of Mediterranean back-arc basins.

232 These reconstructions show that, during 140 Ma, Africa has been mostly under  
233 extension and the subduction zone north of it has been forming back-arc basins, except during  
234 two periods: (1) a first ~25 Myrs long period (100-75 Ma) of compression associated with



235 obduction, propagating away from the obduction zone within Africa and Europe in the Late  
236 Cretaceous and culminating in the Santonian, and, after a period of quiescence from 65 to 45  
237 Ma, (2) compression resumed at 45 Ma and persisted until ~35 Ma, mostly in the west, before  
238 extension was again the predominant regime in Africa and Arabia, except within the Arabia-  
239 Eurasia collision zone (Agard et al. 2011; Mouthereau et al. 2012). The intervening  
240 extensional periods were associated with plate fragmentation and the formation of (1) Apulia  
241 and (2) Arabia. The compressional periods thus seem accidental interruptions in a continuous  
242 process of extension and fragmentation of Africa during its motion toward Eurasia. During  
243 the Mesozoic this succession of extension and compression/obduction thus occurred at least  
244 twice: (1) rifting of Adria/Apulia away from Africa around 180-170 Ma, followed by the  
245 Dinaric obduction between 170 and 150 Ma and (2) distributed extension in Africa in the  
246 Early Cretaceous followed by compression/obduction in the Late Cretaceous. The separation  
247 of Arabia from Africa from the Late Eocene onwards seems the repetition of the same  
248 process, but very little oceanic lithosphere is left and collision occurs coevally (Jolivet and  
249 Faccenna 2000).

250 One important additional observation is that the newly created subduction zones leading  
251 to obduction dipped everywhere toward the north, with the same orientation as the already  
252 existing subduction zones beneath Eurasia, resulting in a totally asymmetrical situation where  
253 the continental lithosphere subducted northward below oceanic lithosphere, while the  
254 classical view would be that the oceanic lithosphere sinks below the continental lithosphere,  
255 whatever the polarity of subduction.

256

### 257 **3. Africa from mantle plumes to subduction**

258

259 During this evolution, several mantle plume events and associated large igneous provinces  
260 (LIPS) are recognized (Fig. 3), from the Central Atlantic Magmatic Province (CAMP) at 200  
261 Ma (Marzoli et al. 1999), the Karoo event some 183-182 Ma ago (Riley et al. 2004; Svensen  
262 et al. 2012), the Etendeka LIPS between 135 and 130 Ma (Turner et al. 1994; Dodd et al.  
263 2015), the Madagascar-Agulhas LIPS around 100 Ma within a greater Southeast African LIP  
264 (Gohl et al. 2011) and finally the Afar volcanism ~45 to 30 Ma ago (Hofmann et al. 1997;  
265 Ershov and Nikishin 2004) further north and the subsequent northward migration of intraplate  
266 volcanism across the western Arabian plate and eastern Anatolia (Courtillot et al. 1999;  
267 Faccenna et al. 2013b; Gaina et al. 2013). The Madagascar-Agulhas LIP, in particular, has  
268 been present offshore South Africa from ~140 to 95 Ma (Gohl et al. 2011). These successive

269 volcanic events sign the presence of a long-lasting mantle upwelling underneath South Africa  
270 during a long period, also responsible for the evolution of dynamic topography in eastern  
271 Africa (Burke 1996; Burke et al. 2008; Moucha and Forte 2011, Torsvik et al. 2014). This  
272 conclusion is further corroborated by the occurrence of kimberlites from ~200 to ~50 Ma with  
273 a younging from east to west (Jelsma et al. 2009; 2004; Torsvik et al. 2010) suggesting that  
274 South Africa has slowly overridden the plume, before the latter migrated northward (Braun et  
275 al. 2014). The plume influence is also suggested by erosion and uplift of the Southern African  
276 Plateau in the Late Cretaceous (Fig. 2-16; MacGregor 2010; Guillocheau et al. 2012; Colli et  
277 al. 2014). Similar uplift and erosion is also recorded in West Africa (Leprêtre et al. 2014).  
278 Frizon de Lamotte et al. (2015) have recently discussed the different styles of rifting that led  
279 to the fragmentation of Gondwana, emphasizing the difference between “passive” rifting  
280 episodes (the rift is localized by inherited structures) and “active” ones (the rift is localized by  
281 the plume that weakens the lithosphere) temporally related to evidence of plume activity. This  
282 new understanding derives from modelling by Burov and Gerya (2015) showing that a plume  
283 cannot trigger a rifting without external extensional forces as it was previously supposed by  
284 Sengör and Burke (1978). The Karoo LIPS (Fig. 3) at 183 Ma is associated with an episode of  
285 rifting leading to the opening of West Indian Ocean. Similarly, the Early Cretaceous rifting  
286 episode can be seen as a consequence of the Parana-Etendeka LIPS.

287 From the Late Cenomanian until the Eocene, the northern part of Africa was under sea water  
288 and subsiding with a decrease at the Paleocene-Eocene boundary (Guiraud et al. 2005;  
289 Swezey 2009). Africa thus shows in the Late Cretaceous and early Cenozoic subsidence of  
290 the northern regions in the vicinity of the subduction and uplift in the south above mantle  
291 plumes. Convergence is accommodated by several subduction zones, one along the southern  
292 margin of Eurasia and two others where continental lithosphere underthrusts oceanic  
293 lithosphere, which all show the same asymmetry with the southern plate underthrusting the  
294 northern one.

295 A horizontal tomographic section (Becker and Boschi 2002) (Fig. 3) in the lower mantle  
296 (1000 km) distinctly shows the plume now sitting below eastern Africa at this depth. It also  
297 shows cold material further north, interpreted as remnants of the Neo-Tethys slab in the lower  
298 mantle (Ricard et al. 1993; Lithgow-Bertelloni and Silver 1998; Ritsema et al. 1999;  
299 Van der Voo et al. 1999 ; Steinberger 2000; Burke and Torsvik 2004; McNamara and Zhong  
300 2005; Hafkenscheid et al. 2006; Garnero and McNamara 2008; van der Meer et al. 2010;  
301 Faccenna et al. 2013a) from the eastern Mediterranean region to India and Indonesia, signing

302 the place where the slab has penetrated the upper-lower mantle transition zone. The timing of  
303 full penetration across the transition zone can be loosely bracketed by matching  
304 reconstructions and tomographic images (backward reconstructions of the slabs seen on  
305 tomographic models) between 70 and 45 Ma with probable significant error bars (Faccenna et  
306 al. 2013a; Replumaz et al. 2013).

307 The Eocene compression has more limited effects compared to the Late Cretaceous one  
308 and these are mostly restricted to the western end of the convergence system, with, however,  
309 the reactivation of earlier extensional structures in the east (Arsenikos et al. 2013).  
310 Nevertheless, the effects of compression are felt over a large domain from the Atlas  
311 Mountains to the Pyrenees (Frizon de Lamotte et al. 2000; Vergès et al. 2002; Mouthereau et  
312 al. 2014). This compression ended at ~35 Ma, when the subduction regime changed and back-  
313 arc extension started (Jolivet and Faccenna 2000).

314

#### 315 **4. Plate velocities**

316

317 The two successive periods of compression (100-75 Ma and 45-35 Ma) correspond to  
318 faster convergence between Africa and Eurasia (fig. 2-13). They are separated during the  
319 Paleocene by a period of very slow convergence (Fig. 2-10, Rosenbaum et al., 2002). The  
320 progressive build-up of Late Cretaceous compression is also coeval with an increase of the  
321 Africa absolute velocity (Fig. 2-11, Gaina et al., 2013), as well as a maximum of sea level at  
322 global scale (Fig. 2-7, Müller et al. 2008). It is also contemporaneous with higher velocities of  
323 spreading in the South Atlantic (Fig. 2-2b). The absolute motion of Africa gradually increased  
324 from the time of emplacement of the Parana-Etendeka LIP in the southern Atlantic to the  
325 emplacement of the Madagascar-Aghulas LIP in the Indian Ocean (Fig. 2-11, Gaina et al.  
326 2013). After this period, the absolute motion of Africa slowed down before a new peak before  
327 30 Ma and a new decrease afterward. The peak of convergence velocity predates the peak of  
328 absolute velocity (Fig. 2-10, 2-11 and 2-13). Faster African plate motion is associated with a  
329 period of increased spreading rate between 120 and 70 Ma in the southern Atlantic (Fig. 2-2  
330 and 2-2b, Cogné and Humler 2006, Conrad and Lithgow-Bertelloni 2007; Colli et al. 2014),  
331 although the global peak of oceanic crust production is recorded earlier at 120 Ma coeval with  
332 the Pacific superplume (Fig. 2-3; Larson 1991; Conrad and Lithgow-Bertelloni 2007).  
333 Subduction initiation in the Tethys Ocean in the Late Cretaceous, as shown by the age of  
334 metamorphic soles beneath ophiolites (Figs. 2-21, 2-22, 2-23) temporally coincides with the  
335 period of increasing absolute velocity and the peak of convergence velocity (see green-shaded

336 periods in figure 2). Similarly, the peak of Indian Plate velocity (Fig. 2-14 and 2-15)  
337 coincides with the age of metamorphic sole below ophiolites obducted onto the northern and  
338 western margins of India and the age of the Southwest Indian plume at the very end of the  
339 Cretaceous (Gnos et al. 1997).

340

## 341 **5. Discussion**

342

343 In a recent paper, Sengör and Stock (2014) have analysed the Late Cretaceous  
344 compressional episode along the northern margin of Africa and proposed the name of  
345 Ayyubid Orogen. In their interpretation, the eastern part of this orogen, equivalent to the  
346 “Croissan Ophiolitique Péri-Arabe” of Ricou (1971), results from the obduction of the Tethys  
347 oceanic floor, while the western part results from an aborted obduction. They have analyzed  
348 the kinematic changes in the motion of Africa and conclude that the Ayyubid Orogen started  
349 to form before the kink in the motion path of Africa at 84 Ma (see also figure 1C and 1D),  
350 which implies that some other cause should be investigated. This also shows that the state of  
351 stress in the subducting plate is not simply related to the direction of convergence between  
352 Africa and Eurasia. They further propose that one has to invoke the plates that were lost  
353 during the convergence process, but do not put forward an explanation for the change in stress  
354 regime that finally led to the observed obduction. The data compiled here illustrate that  
355 obduction is a large-scale tectonic process completed within a short time frame. One may then  
356 speculate that it is related to a large geodynamic cause, involving changes in subduction  
357 dynamics, increase plume activity and plate velocity increase and not only to local plate  
358 motion re-orientation. Vaughan and Scarrow (2003) proposed for instance that obduction can  
359 be linked to superplumes events producing compression over the entire subduction system.  
360 The period of compression in the Late Cretaceous, including obduction, is indeed coeval with  
361 faster convergence, increase of the absolute motion of Africa and interaction with super  
362 plumes. Recent studies have shown the importance of mantle plumes in governing the mantle  
363 flow beneath Africa and supporting its topography (Forte et al. 2010; Glisovic et al. 2012;  
364 Moucha and Forte 2011; Glisovic and Forte 2014). Large-scale mantle plumes emanating  
365 from large low-shear velocity provinces in the lower mantle, one below South Africa and one  
366 below the Pacific (Behn et al. 2004; Torsvik et al. 2006; Burke 2011; Bower et al. 2013) are  
367 thought to be stable over tens or hundreds of Myrs (Glisovic et al. 2012; Bower et al. 2013)  
368 suggesting a rather stable pattern of convection in the mantle. Strain pattern in the mantle  
369 below Africa, deduced from SKS seismic anisotropy, is furthermore compatible with

370 northward mantle flow related to the African superplume (Bagley and Nyblade 2013; Hansen  
371 et al. 2012). Similarly, the northward motion of Arabia, after its separation from Africa some  
372 30 Ma ago and the migration of hotspot-related volcanism toward the collision zone are also  
373 compatible with a northward asthenospheric flow dragging Africa and Arabia (Faccenna et al.  
374 2013b). Plume drag/push efficiency is attested by the fact that the motion of Arabia did not  
375 stop after collision although there is no longer any significant slab to power its northward  
376 motion (McQuarrie et al. 2003; Alvarez 2010; Faccenna et al. 2013b).

377 Recent analogues experiments (Agard et al. 2014; Edwards et al. 2015) suggest that  
378 subducting a continental margin below a denser oceanic lithosphere is feasible once  
379 subduction has initiated, which remains the main problem. In a set of models comparable to  
380 the Tethyan system, Agard et al. (2014) show that the jamming of the northern subduction can  
381 lead to subduction initiation further south, leading to obduction on the African margin,  
382 reemphasizing the model proposed by Agard et al. (2007) in which faster plate velocity  
383 renders subduction more difficult, putting the system in compression and inducing the  
384 formation of a new subduction zone.

385 Elaborating on the ideas suggested by Vaughan and Scarrow (2003) we now discuss a  
386 new plausible scenario coupling the evolution of the Tethyan subduction with a super plumes  
387 below South Africa (Fig. 4) that should take into account three main large-scale observations:  
388 (1) the repeated detachment of continental pieces from Africa in the north, (2) the  
389 contemporaneity of faster Africa motion, plume activity in the south and  
390 compression/obduction and (3) the systematic southward polarity of obduction (northward  
391 subduction).

392 Step 1 (Figure 4A): Assuming a continuous northward asthenospheric flow, which the  
393 superplume is part of, since the Jurassic, we first propose that extension and fragmentation of  
394 Africa (in the middle Jurassic and “middle” Cretaceous) result from this flow and the shear, or  
395 the push, it imposes to the base of the lithosphere (Bott 1993; Ziegler 1992; Stoddard and  
396 Abott 1996). Africa was thus driven both by this drag/push and by slab pull in the subduction  
397 zone below Eurasia through a convective conveyor belt. We speculate that as long as the  
398 continuity of the conveyor belt existed, plume push resulted in extension episodes and  
399 sometimes in the stripping of microcontinents in the north of Africa. This hypothesis offers  
400 the advantage of explaining the repetition of the same process above a continuous northward  
401 mantle flow from the Paleozoic to the present, if Africa has been all along under the influence  
402 of mantle flow largely controlled by a long-lasting plume. Before plate acceleration and  
403 compression, the slab was not restricted to the upper mantle and partly retreated southward,

404 leading to back-arc rifting in the upper Eurasian plate (Black Sea; South Caspian; Nain-Baft,  
405 Sabzevar and possibly Sistan in Central Iran).

406 Step 2 (Figure 4B): Obduction. Interactions of mantle flow and cratonic lithospheric  
407 keels has long been discussed (Stoddard and Abbott 1996) and it has been recently suggested  
408 that continental cratonic keels may lead to plate acceleration when a plume arrives (Zahirovic  
409 et al. 2015). The detailed interactions between a plume and a continent above are not known  
410 but some recent investigations by Koptev et al. (2015) have confirmed the early work of  
411 Stoddard and Abott (1996) and the importance of the push of the plume of the irregularities of  
412 the base of the lithosphere to move continents. Following up on this suggestion, we propose  
413 that the push due to the African superplume forced the (African) slab beneath Eurasia into the  
414 upper mantle at a faster rate. Slab penetration in the lower mantle could have produced a  
415 surge of compression within the subducting plate, leading to the formation of a new  
416 subduction zone close to the North African margin (figs. 4B). Stresses would then build up  
417 until the whole system is in compression, leading to the so-called Santonian event. The Late  
418 Cretaceous compression is associated with an uplift of South Africa when it passes above the  
419 plume, while North Africa is instead subsiding and subducting below the obducting Tethys  
420 oceanic lithosphere. A mechanical link between slab penetration and the progressive  
421 reorientation of the Africa-Eurasia convergence around 84 Ma should be studied.

422 Step 3 (Figure 4C): These compressional stresses would then be relaxed once the  
423 penetration beneath Eurasia is complete in the lower mantle and the conveyor belt is restored,  
424 that is some 70 Ma ago, when the Neo-Tethys obduction process stopped. The 25 Myrs of  
425 compression would then be the time needed from plate acceleration to full slab penetration  
426 into the lower mantle. The same process may have happened again further east at the very end  
427 of the Cretaceous with the obduction of ophiolites on top of the northern and western margins  
428 of India. It may also have happened earlier at the end of the Jurassic to form the Dinaric  
429 ophiolite.

430 The boundary conditions of the model would then be radically different before and  
431 during the compressional episode. Before compression the plume in the south pushes on a  
432 plate that is free to move northward on its northern boundary and the system is driven by slab  
433 pull that is more efficient than plume push. During compression the more active plume  
434 induces a stronger push in the south while the slab is penetrating the upper-lower mantle  
435 discontinuity in the north, thus inducing compression in the whole northern half of the  
436 African plate.



437 This scenario can furthermore create the asymmetrical boundary conditions explaining  
438 the polarity of the newly created subductions and the underthrusting of old and dense  
439 continental mantle below younger and lighter oceanic mantle. We show in figure 5 a possible  
440 evolution at the start of obduction, shortly after a young oceanic domain had formed (hence  
441 before compression started). The mantle flow dragging, or pushing, Africa northward imposes  
442 a general shear sense such that the newly created subduction is dipping north, leading to the  
443 underthrusting of the African margin and continental domain, supported by an old and cold  
444 lithospheric mantle, below the young and hot oceanic domain newly formed.

445 Step 4 (Figure 4D): In the eastern part of the system the conveyor belt is active between  
446 the slab penetrating deep in the mantle in the north and the plume pushing the African plate  
447 toward the north. The situation is quite similar to the Jurassic stage with this time extension  
448 active in the future Gulf of Aden and Red Sea and the separation of Arabia from Africa.  
449 Back-arc extension is active in the Mediterranean. In the west, compression resumed in the  
450 Eocene in Africa and the most significant compressional tectonics is restricted to the western  
451 half of the system, especially in the Atlas system, with also some inversion of extensional  
452 features farther east from Cyrenaica to the Palmyrides. This new compressional period is  
453 coeval with the building of the Hellenides-Taurides accretionary wedge at the expense of the  
454 Pindos Ocean and then the northern margin of Apulia. In the westernmost Mediterranean,  
455 compression is active from the Atlas to the Pyrenees and the question of stress propagation  
456 from Africa to Eurasia must be discussed. If collision was already going on in the future  
457 Gibraltar Arc (Jolivet and Faccenna 2000; Jolivet et al. 2003), compressional stresses were  
458 transmitted across the collision zone within the lithosphere from the Atlas to the Pyrenees. If  
459 one assumes instead that collision was not yet effective and that some narrow oceanic domain  
460 was still present between Africa and Iberia (Vergés and Sabat 1999; Frizon de Lamotte et al.  
461 2000), the compressional stress regime before 35 Ma may be due to the progressive formation  
462 of the subduction zone since the Late Cretaceous, very slow in the first period and then  
463 becoming mature enough for arc volcanism to develop and slab pull to be active and  
464 accommodate slab retreat after 35-30 Ma. The slight velocity increase of the absolute motion  
465 of Africa seen in some kinematic models between 40 and 30 Ma may also suggest that  
466 coupling with the Afar plume when it impacted the base of the African lithosphere has  
467 accelerated the displacement of Africa before the effective collision in the Caucasus-Zagros  
468 region that slowed it drastically.

469 An alternative scenario was recently discussed by Jagoutz et al. (2015) to explain the  
470 velocity increase of the India-Asia convergence in the Latest Cretaceous, involving a double



471 subduction north of India. The southernmost of these two subduction zones in the west is  
472 equivalent to the obduction zone in our model. So the geometry is similar in the two models  
473 and Jagoutz et al. (2015) argue through numerical modelling that this double subduction is  
474 likely to have accelerated convergence but they do not address the question of the initiation of  
475 this subduction zone, which is the topic of the present paper, nor do they explain the observed  
476 polarity of subduction.

477

## 478 **6. Conclusion**

479

480 Our scenario aims at integrating large-scale tectonic processes within a progressive  
481 evolution of the convergence zone between Africa and Eurasia. Because the scale of plate  
482 fragmentation and subsequent obduction is so large, we look for processes involving the  
483 whole mantle. We stress that the Late Cretaceous compression cannot have been a  
484 consequence of continental collision since the Neo-Tethys Ocean was still widely open when  
485 it happened. We propose that the alternation of periods of extension and compression  
486 (including obduction) in Africa and the Neo-Tethys Realm result from changes in the  
487 dynamics of convection underneath, combined with regional-scale reorganizations. The long-  
488 term geological record suggests that the normal extensional situation corresponds to steady-  
489 state whole-mantle convection, Africa being carried northward by a large-scale conveyor belt,  
490 through plume push in the south and slab pull in the north, while the Late Cretaceous  
491 compression and obduction would result from plate acceleration due to increasing plume push  
492 below South Africa and difficult penetration before slab avalanching in the lower mantle,  
493 until full penetration of the Tethyan slab across the transition zone and reestablishment of the  
494 conveyor belt. This would have produced a strong compression at plate boundaries and, as a  
495 consequence, would have activated a new plate boundary at the location of previous crustal  
496 weakness (Agard et al. 2014). The asymmetry of the northward mantle flow may explain the  
497 polarity of initiation of a northward subduction, leading to obduction with oceanic crust  
498 emplaced on top of the subducting continental margins of Africa and Apulia through basal  
499 drag or push. Although the scale of the obduction at the Jurassic-Cretaceous boundary in the  
500 Dinarides cannot compare with the Late Cretaceous one, a similar scenario could be  
501 envisaged. The later Eocene compression would be the consequence of either subduction  
502 initiation in the Western Mediterranean or plate collision. As super plumes and subduction  
503 zones, which govern mantle convection, are long-lived features, testing models of mantle  
504 convection requires using sequences of events on long durations that only the geological

505 record is able to provide. Such scenarios can be useful to modellers as they may provide time  
506 constants (~20 My) for the establishment/destruction of whole-mantle convection cells or slab  
507 penetration in the lower mantle.

508

509

510 **Acknowledgments:** This article is a contribution of the ERC Advanced Research Grant  
511 n° 290864 (RHEOLITH), of Labex VOLTAIRE and Institut Universitaire de France.

512

Draft

513 **References**

514

515 Abadi, A.M., van Wees, J.D., van Dijk, P.M., Cloetingh, S.A.P.L., 2008. Tectonics and  
516 subsidence evolution of the Sirt Basin, Lybia. AAPG Bulletin 92, 993-1027.

517 Agard, P., Jolivet, L., Vrielynck, B., Monié, P., Burov, E., 2007. Plate accelerations: the  
518 obduction trigger? Earth Planet. Sci. lett. 258, 428-441.

519 Agard, P., Monié, P., Gerber, W., Omrani, J., Molinaro, M., Labrousse, L., Vrielynck, B.,  
520 Meyer, B., Jolivet, L., Yamato, P., 2006. Transient, syn-obduction exhumation of  
521 Zagros blueschists inferred from P-T -t and kinematic constraints: Implications for  
522 Neotethyan wedge dynamics. J. Geophys. Res. 111, doi:10.1029/2005JB004103.

523 Agard, P., Omrani, J., Jolivet, L., Mouthereau, F., 2005. Convergence history across Zagros  
524 (Iran): constraints from collisional and earlier deformation. Int Jour. Earth Sci. 94, 401-  
525 419, DOI 410.1007/s00531-00005-00481-00534.

526 Agard, P., Omrani, J., Jolivet, L., Whitechurch, H., Vrielynck, B., Spakman, W., Monié, P.,  
527 Meyer, B., Wortel, R., 2011. Zagros orogeny: a subduction-dominated process. Geol.  
528 Mag., doi:10.1017/S001675681100046X.

529 Agard, P., Zuo, X., Funicello, F., Bellahsen, N., Faccenna, C., Savva, D., 2014. Obduction:  
530 Why, how and where. Clues from analog models. Earth Planet. Sci. lett. 393, 132-145.

531 Ait-Hamou, F., 2006. Le volcanisme cénozoïque à l'échelle du bombement de l'Ahaggar  
532 (Sahara Central algérien): synthèse géochronologique et répartition spatio-temporelle.  
533 Quelques implications en relation avec l'histoire eo-alpine de la plaque Afrique. Mem.  
534 Serv. Géol. Nation. 13, 155-167.

535 Alvarez, W., 2010. Protracted continental collisions argue for continental plates driven by  
536 basal traction. Earth Planet. Sci. lett. 296, 434-442,  
537 doi:410.1016/j.epsl.2010.1005.1030.

538 Angiboust, S., Agard, P., De Hoog, J.C.M., Omrani, J., Plunder, A., 2013. Insights on deep,  
539 accretionary subduction processes from the Sistan ophiolitic "mélange" (Eastern Iran).  
540 Lithos 156-159, 139-158.

541 Angiboust, S., Agard, P., Jolivet, L., Beyssac, O., 2009. The Zermatt-Saas ophiolite: the  
542 largest (60-km wide) and deepest (c. 70–80 km) continuous slice of oceanic lithosphere  
543 detached from a subduction zone? . Terra Nova 21, 171-180, doi: 110.1111/j.1365-  
544 3121.2009.00870.x.

545 Arsenikos, S., Frizon de Lamotte, D., Chamot-Rooke, N., Mohn, G., Bonneau, M.C.,  
546 Blanpied, C., 2013. Mechanism and timing of tectonic inversion in Cyrenaica

- 547 (Libya): Integration in the geodynamics of the East Mediterranean. *Tectonophysics* 608,  
548 319-329, <http://dx.doi.org/310.1016/j.tecto.2013.1009.1025>.
- 549 Bagley, B., Nyblade, A.A., 2013. Seismic anisotropy in eastern Africa, mantle flow, and the  
550 African superplume. *Geophys. Res. Lett.* 40, 1500-1505, doi:1510.1002/grl.50315.
- 551 Barrier, E., Vrielynck, B., 2008. *Paleotectonic Maps of the Middle East: Atlas of 14 Maps*,  
552 Paris.
- 553 Becker, T.W., Boschi, L., 2002. A comparison of tomographic and geodynamic mantle  
554 models. *Geochem. Geophys. Geosyst* 3, 10.129/2001GC000168.
- 555 Behn, M.D., Conrad, C.P., Silver, P.G., 2004. Detection of upper mantle flow associated with  
556 the African Superplume. *Earth Planet. Sci. Lett.* 224, 259–274,  
557 doi:210.1016/j.epsl.2004.1005.1026.
- 558 Bellahsen, N., Faccenna, C., Funiciello, F., Daniel, J.M., Jolivet, L., 2003. Why did Arabia  
559 separate from Africa, insights from 3-D laboratory experiments. *Earth Planet. Sci. Lett.*  
560 216, 365-381.
- 561 Benkhelil, J., 1989. The origin and evolution of the Cretaceous Benue Trough (Nigeria).  
562 *Journal of African Earth Sciences* 8, 251-282.
- 563 Benkhelil, J., Dainelli, P., Ponsard, J.F., Popoff, M., Saugy, L., 1988. The Benue Trough:  
564 wrench-fault related basin on the border of the equatorial Atlantic, in: Manspeizer, W.  
565 (Ed.), *Triassic-Jurassic rifting. Continental breakup and the origin of the Atlantic Ocean*  
566 *and passive margins. Part A.* Elsevier, Amsterdam, pp. 787-819.
- 567 Bevan, T.G., Moustafa, A.R., 2012. Inverted rift-basins of Northern Egypt, in: Roberts, D.G.,  
568 Bally, A.W. (Eds.), *Regional geology and tectonics: Phanerozoic rift systems and*  
569 *sedimentary basins.* Elsevier, Amsterdam, pp. 483-507.
- 570 Bosworth, W., Guiraud, R., Kessler, L.G., 1999. Late Cretaceous (ca. 84 Ma) compressive  
571 deformation of the stable platform of northeast Africa (Egypt): Far-field stress effects of  
572 the “Santonian event” and origin of the Syrian arc deformation belt. *Geology* 27, 633-  
573 636.
- 574 Bott, M.H.P., 1993. Modelling the plate-driving mechanism. *Journal of the Geological*  
575 *Society* 150, 941-951.
- 576 Bower, D.J., Gurnis, M., Seton, M., 2013. Lower mantle structure from paleogeographically  
577 constrained dynamic Earth models. *Geochem. Geophys. Geosyst* 14, 44-63,  
578 doi:10.1029/2012GC004267.

- 579 Braun, J., Guillocheau, F., Robin, C., Baby, G., Jelsma, H., 2014. Rapid erosion of the  
580 Southern African Plateau as it climbs over a mantle superswell. *J Geophys. Res.* 119,  
581 6093–6112, doi:6010.1002/2014JB010998.
- 582 Burke, K., 1996. The African Plate. *S. Afr. J. Geol.* 99, 341-409.
- 583 Burke, K., 2011. Plate Tectonics, the Wilson Cycle, and Mantle Plumes: Geodynamics from  
584 the Top. *Annu. Rev. Earth Planet. Sci.* 39, 1-29.
- 585 Burke, K., Gunnell, Y., 2008. The African erosion surface: a continental-scale synthesis of  
586 geomorphology, tectonics and environmental changes over the past 180 million years.  
587 *Memoirs of the Geological Society of America* 201, 66 p.
- 588 Burke, K., MacGregor, D.S., Cameron, N.R., 2003. Africa's Petroleum systems: four tectonic  
589 Aces in the past 600 million years, in: Arthur, T.J., MacGregor, D.S., Cameron, N.R.  
590 (Eds.), *Petroleum Geology of Africa: New Themes and Developing Technologies*. The  
591 Geological Society of London, London, pp. 21-60.
- 592 Burke, K., Steinberger, B., Torsvik, T.H., Smethurst, M.A., 2008. Plume Generation Zones at  
593 the margins of Large Low Shear Velocity Provinces on the core–mantle boundary.  
594 *Earth and Planetary Science Letters* 265, 49–60, doi:10.1016/j.epsl.2007.1009.1042.
- 595 Burke, K., Torsvik, T.H., 2004. Derivation of Large Igneous Provinces of the past 200 million  
596 years from long-term heterogeneities in the deep mantle. *Earth Planet. Sci. lett.* 227,  
597 531–538.
- 598 Burov, E., Gerya, T., 2014. Asymmetric three-dimensional topography over mantle plumes.  
599 *Nature* 513, 85-89, doi:10.1038/nature13703.
- 600 Çelik, Ö.F., Delaloye, M., Feraud, G., 2006. Precise  $^{40}\text{Ar}$ – $^{39}\text{Ar}$  ages from the metamorphic  
601 sole rocks of the Tauride Belt ophiolites, southern Turkey: implications for the rapid  
602 cooling history. *Geological Magazine* 143, 213–227.
- 603 Celik, O.F., Marzoli, A., Marschik, R., Chiaradia, M., Neubauer, F., Öz, I., 2011. Early–  
604 Middle Jurassic intra-oceanic subduction in the İzmir-Ankara-Erzincan Ocean, Northern  
605 Turkey. *Tectonophysics* 509, 120–134, doi:110.1016/j.tecto.2011.1006.1007.
- 606 Cogné, J.P., Humler, E., 2006. Trends and rhythms in global seafloor generation rate.  
607 *Geochem. Geophys. Geosyst* 7, Q03011, doi:03010.01029/02005GC001148.
- 608 Coleman, R.G., 1977. *Ophiolites*. Springer Verlag, Berlin.
- 609 Coleman, R.G., 1981. Tectonic setting for ophiolite obduction in Oman. *J. Geophys. Res.* 86,  
610 2497-2508.
- 611 Colli, L., Stotz, I., Bunge, H.P., Smethurst, M., Clark, S., Iaffaldano, G., Tassara, A.,  
612 Guillocheau, F., Bianchi, M.C., 2014. Rapid South Atlantic spreading changes and

- 613 coeval vertical motion in surrounding continents: Evidence for temporal changes of  
614 pressure-driven upper mantle flow. *Tectonics* 32, 1304-1321,  
615 doi:1310.1002/2014TC003612.
- 616 Conrad, C.P., Lithgow-Bertelloni, C., 2007. Faster seafloor spreading and lithosphere  
617 production during the mid-Cenozoic. *Geology* 35, 29–32; doi:  
618 10.1130/G22759A.22751.
- 619 Courtillot, V., Jaupart, C., Manighetti, I., Tapponnier, P., Besse, J., 1999. On causal links  
620 between flood basalt and continental breakup. *Earth Planet. Sci. Lett.* 166, 177-195.
- 621 Dercourt, J., Zonenshain, L.P., Ricou, L.E., Kuzmin, V.G., Le Pichon, X., Knipper, A.L.,  
622 Grandjacquet, C., Sbertshikov, I.M., Geysant, J., Lepvrier, C., Pechersky, D.H.,  
623 Boulin, J., Sibuet, J.C., Savostin, L.A., Sorokhtin, O., Westphal, M., Bazhenov, M.L.,  
624 Lauer, J.P., Biju-Duval, B., 1986. Geological evolution of the Tethys belt from the  
625 Atlantic to the Pamir since the Lias. *Tectonophysics* 123, 241-315.
- 626 Dewey, J.F., 1976. Ophiolite obduction. *Tectonophysics* 31, 93-120.
- 627 Dewey, J.F., Casey, J.F., 2013. The sole of an ophiolite: the Ordovician Bay of Islands  
628 Complex, Newfoundland. *J. Geol. Soc London* 170, 715-722,  
629 dx.doi.org/710.1144/jgs2013-1017.
- 630 Dodd, S.C., Mac Niocaill, C., Muxworthy, A.R., 2015. Long duration (>4 Ma) and steady-  
631 state volcanic activity in the early Cretaceous Paraná–Etendeka Large Igneous  
632 Province: New palaeomagnetic data from Namibia. *Earth Planet. Sci. Lett.* 414, 16-29,  
633 <http://dx.doi.org/10.1016/j.epsl.2015.1001.1009>.
- 634 Doubrovine, P., Steinberger, B., Torsvik, T.H., Absolute plate motions in a reference frame  
635 defined by moving hotspots in the Pacific, Atlantic and Indian oceans. *J. Geoph. Res.*  
636 117, B09101, <http://dx.doi.org/09110.01029/02011JB009072>.
- 637 Edwards, S.J., Schellart, W.P., Duarte, J.C., 2015. Geodynamic models of continental  
638 subduction and obduction of overriding plate forearc oceanic lithosphere on top of  
639 continental crust. *Tectonics*, DOI: 10.1002/2015TC003884.
- 640 Ershov, A.V., Nikishin, A.M., 2004. Recent geodynamics of the Caucasus–Arabia–East  
641 Africa Region. *Geotectonics*, Engl. Transl. 38 123–136.
- 642 Faccenna, C., Becker, T.W., Conrad, C.P., Husson, L., 2013a. Mountain building and mantle  
643 dynamics. *Tectonics* 32, 80–93, doi:10.1029/2012TC003176.
- 644 Faccenna, C., Becker, T.W., Jolivet, L., Keskin, M., 2013b. Mantle convection in the Middle  
645 East: Reconciling Afar upwelling, Arabia indentation and Aegean trench rollback. *Earth  
646 Planet. Sci. Lett.* 375, 254-269; dx.doi.org/210.1016/j.epsl.2013.1005.1043.

- 647 Forte, A.M., Quéré, S., Moucha, R., Simmons, N.A., Grand, S.P., Mitrovica, J.X., Rowley,  
648 D.B., 2010. Joint seismic–geodynamic–mineral physical modelling of African  
649 geodynamics: A reconciliation of deep-mantle convection with surface geophysical  
650 constraints. *Earth Planet. Sci. Lett.* 295, 329–341, doi:10.1016/j.epsl.2010.1003.1017.
- 651 Frizon de Lamotte, D., Fourdan, B., Leleu, S., Leparmentier, F., de Clarens, P., 2015. Style of  
652 rifting and the stages of Pangea breakup. *Tectonics* 34, 1009–1029,  
653 doi:10.1002/2014TC003760.
- 654 Frizon de Lamotte, D., Raulin, C., Mouchot, N., Wrobel - Daveau, J.C., Blanpied, C.,  
655 Ringenbach, J.C., 2011. The southernmost margin of the Tethys realm during the  
656 Mesozoic and Cenozoic: Initial geometry and timing of the inversion processes.  
657 *Tectonics* 30, TC3002, doi:10.1029/2010TC002691.
- 658 Frizon de Lamotte, D., Saint Bezar, B., Bracène, R., Mercier, E., 2000. The two main steps of  
659 the Atlas building and geodynamics of the West Mediterranean. *Tectonics* 19, 740–761.
- 660 Gaina, C., Torsvik, T.H., van Hinsbergen, D.J.J., Medvedev, S., Werner, S.C., Labails, C.,  
661 2013. The African Plate: A history of oceanic crust accretion and subduction since the  
662 Jurassic. *Tectonophysics* 604, 4–25, <http://dx.doi.org/10.1016/j.tecto.2013.1005.1037>.
- 663 Garnero, E.J., McNamara, A.K., 2008. Structure and dynamics of the Earth's lower mantle.  
664 *Science* 320, 626–628.
- 665 Gass, I.G., 1968. Is the Troodos Massif of Cyprus a fragment of Mesozoic ocean floor ?  
666 *Nature* 220, 39–42.
- 667 Genik, G.J., 1993. Petroleum geology of Cretaceous-Tertiary rift basins in Niger, Chad, and  
668 Central African Republic. *AAPG Bulletin* 77, 1405–1434.
- 669 Glisovic, P., Forte, A.M., 2014. Reconstructing the Cenozoic evolution of the mantle:  
670 Implications for mantle plume dynamics under the Pacific and Indian plates. *Earth*  
671 *Planet. Sci. Lett.* 390, 146–156, <http://dx.doi.org/10.1016/j.epsl.2014.1001.1010>.
- 672 Glisovic, P., Forte, A.M., Moucha, R., 2012. Time-dependent convection models of mantle  
673 thermal structure constrained by seismic tomography and geodynamics: implications for  
674 mantle plume dynamics and CMB heat flux. *Geophys. J. Int.* 190, 785–815 doi:  
675 10.1111/j.1365-1246X.2012.05549.x.
- 676 Gnos, E., Immenhauser, A., Peters, T., 1997. Late Cretaceous/early Tertiary convergence  
677 between the Indian and Arabian plates recorded in ophiolites and related sediments.  
678 *Tectonophysics* 271, 1–19.

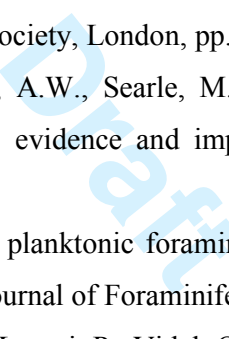


- 679 Goffé, B., Michard, A., Kienast, J.R., Le Mer, O., 1988. A case of obduction-related high  
680 pressure, low temperature metamorphism in upper crustal nappes, Arabian continental  
681 margin, Oman: P-T paths and kinematic interpretation. *Tectonophysics* 151, 363-386.
- 682 Gohl, K., Uenzelmann-Neben, G., Grobys, N., 2011. Growth and dispersal of a southeast  
683 African large igneous province. *South African Journal of Geology* 114, 379-386,  
684 doi:10.2113/gssajg.2114.2113-2114.2379.
- 685 Guillocheau, F., Robin, C., Allemand, P., Bourquin, S., Brault, N., Dromart, G., Freidenberg,  
686 R., Garci, J.P., Gaulier, J.M., Gaumet, F., Grosdoy, B., Hanot, F., Le Strat, P., Mettraux,  
687 M., Nalpas, T., Prijac, C., Rigollet, C., Serrano, O., Grandjean, G., 2000. Meso-  
688 cenozoic geodynamic evolution of the Paris basin, stratigraphic constraints.  
689 *Geodynamica Acta* 13, 189-246.
- 690 Guillocheau, F., Rouby, D., Robin, C., Helm, C., Rolland, N., Carlier de Veslud, C.L.,  
691 Braunz, J., 2012. Quantification and causes of the terrigenous sediment budget at the  
692 scale of a continental margin: a new method applied to the Namibia-South Africa  
693 margin. *Basin Research* 24, 3–30, doi: 10.1111/j.1365-2117.2011.00511.x.
- 694 Guillot, S., Replumaz, A., 2013. Importance of continental subductions for the growth of the  
695 Tibetan plateau. *Bull Soc géol France* 184, 199-223.
- 696 Guiraud, R., Bosworth, W., Thierry, J., Delplanque, A., 2005. Phanerozoic geological  
697 evolution of Northern and Central Africa: An overview. *Journal of African Earth*  
698 *Sciences* 43, 83–143.
- 699 Hacker, B.R., 1991. The role of deformation in the formation of metamorphic gradients, ridge  
700 subduction beneath the Oman ophiolite. *Tectonics* 10, 455-474.
- 701 Hacker, B.R., Mosenfelder, J.L., Gnos, E., 1996. Rapid emplacement of the Oman ophiolite:  
702 thermal and geochronologic constraints. *Tectonics* 15, 1230-1247.
- 703 Hafkenschied, E., Wortel, M.J.R., Spakman, W., 2006. Subduction history of the Tethyan  
704 region derived from seismic tomography and tectonic reconstructions. *J. Geophys. Res.*  
705 111, doi:10.1029/2005JB003791.
- 706 Hansen, S.E., Nyblade, A.A., Benoit, M.H., 2012. Mantle structure beneath Africa and Arabia  
707 from adaptively parameterized P-wave tomography: Implications for the origin of  
708 Cenozoic Afro-Arabian tectonism. *Earth Planet. Sci. Lett.* 319-320, 23-34,  
709 doi:10.1016/j.epsl.2011.1012.1023.
- 710 Hässig, M., Rolland, Y., Duretz, T., Sosson, M., 2015a. Obduction triggered by regional  
711 heating during plate reorganization. *Terra Nova* in press, doi: 10.1111/ter.12193.

- 712 Hässig, M., Rolland, Y., Sosson, M., Galoyan, G., Avagyan, A., 2015b. P-T-t history of the  
713 Amasia ophiolite 'metamorphic sole' (Armenia, Lesser Caucasus): implications for the  
714 obduction process of an old oceanic lithosphere. in press.
- 715 Hässig, M., Rolland, Y., Sosson, M., Galoyan, G., Müller, C., Avagyan, A., Sahakyan, L.,  
716 2013. New structural and petrological data on the Amasia ophiolites (NW Sevan–Akera  
717 suture zone, Lesser Caucasus): Insights for a large-scale obduction in Armenia and NE  
718 Turkey. *Tectonophysics* 588, 135-153,  
719 <http://dx.doi.org/10.1016/j.tecto.2012.1012.1003>.
- 720 Hippolyte, J.C., Müller, C., Kaymakci, N., Sangu, E., 2010. Dating of the Black Sea Basin:  
721 new nannoplankton ages from its inverted margin in the Central Pontides (Turkey), in:  
722 Sosson, M., Kaymakci, N., Stephenson, R., Bergerat, F., Starostenko, V. (Eds.),  
723 *Sedimentary Basin Tectonics from the Black Sea and Caucasus to the Arabian Platform*.  
724 Geological Society, London, pp. 113-136, DOI: 110.1144/SP1340.1147.
- 725 Hofmann, C., Courtillot, V., Feraud, G., Rochette, P., Yirgu, G., Ketefo, E., Pik, R., 1997.  
726 Timing of the Ethiopian flood basalt event and implications for plume birth and global  
727 change. *Nature* 389, 838–841.
- 728 Jammes, S., Tiberi, C., Manatschal, G., 2010. 3D architecture of a complex transcurrent rift  
729 system: The example of the Bay of Biscay–Western Pyrenees. *Tectonophysics* 489,  
730 210-226, doi:210.1016/j.tecto.2010.1004.1023.
- 731 Jelsma, H., Barnett, W., Richards, S., Lister, G., 2009. Tectonic setting of kimberlites. *Lithos*  
732 112S, 155-165, doi:110.1016/j.lithos.2009.1006.1030.
- 733 Jelsma, H.A., de Wit, M.J., Thiart, C., Dirks, P.H.G.M., Viola, G., Basson, I.J., Anckar, E.,  
734 2004. Preferential distribution along transcontinental corridors of kimberlites and  
735 related rocks of Southern Africa. *South African Journal of Geology* 107, 301-324.
- 736 Jolivet, L., Brun, J.P., 2010. Cenozoic geodynamic evolution of the Aegean region. *Int. J.*  
737 *Earth Science* 99, 109–138, DOI: 110.1007/s00531-00008-00366-00534.
- 738 Jolivet, L., Faccenna, C., 2000. Mediterranean extension and the Africa-Eurasia collision.  
739 *Tectonics* 19, 1095-1106.
- 740 Jolivet, L., Faccenna, C., Goffé, B., Burov, E., Agard, P., 2003. Subduction tectonics and  
741 exhumation of high-pressure metamorphic rocks in the Mediterranean orogens. *Am. J.*  
742 *Science* 303, 353-409.
- 743 Kidd, W.S.F., Dewey, J.F., Bird, J.M., 1978. The Mings Bight Ophiolite Complex,  
744 Newfoundland: Appalachian oceanic crust and mantle. *Can. J. Earth Sci.* 15, 781-804.

- 745 Koptev, A., Calais, E., Burov, E., Leroy, S., Gerya, T., 2015. Dual continental rift systems  
746 generated by plume-lithosphere interaction. *Nature Geoscience* 8, 388-392, DOI:  
747 310.1038/NGEO2401.
- 748 Lardeaux, J.M., Schwartz, S., Tricart, P., Paul, A., Guillot, S., Béthoux, N., Masson, F., 2006.  
749 A crustal-scale cross-section of the south-western Alps combining geophysical and  
750 geological imagery. *Terra Nova* 18, 412-422, doi: 410.1111/j.1365-3121.2006.00706.x.
- 751 Larson, R.L., 1991. Latest pulse of Earth: evidence for a mid-Cretaceous superplume.  
752 *Geology* 19, 547-550.
- 753 Leprêtre, R., Barbarand, J., Missenard, Y., Leparmentier, F., Frizon de Lamotte, D., 2014.  
754 Vertical movements along the northern border of the West African Craton: the Reguibat  
755 Shield and adjacent basins. *Geol. Mag.* 151, 885-898.
- 756 Liégeois, J.P., Benhallou, A., Azzouni-Sekkal, A., Yahiaoui, R., Bonin, B., 2005. The Hoggar  
757 swell and volcanism: Reactivation of the Precambrian Tuareg shield during Alpine  
758 convergence and West African Cenozoic volcanism,, in: Foulger, G.R., Natland, J.H.,  
759 Presnall, D.C., Anderson, D.L. (Eds.), *Plates, plumes, and paradigms*. Geological  
760 Society of America, Boulder, Colorado, pp. 379–400.
- 761 Lithgow-Bertelloni, C., Silver, P.G., 1998. Dynamic topography, plate driving forces and the  
762 African superswell. *Nature* 395, 269–272.
- 763 Macgregor, D., 2010. Understanding African and Brazilian Margin Climate, Topography and  
764 Drainage Systems, Implications for Predicting Deepwater Reservoirs and Source Rock  
765 Burial History. *Search and Discovery Article #90100*.
- 766 MacLeod, C.J., Lissenberg, C.J., Bibby, L.E., 2013. “Moist MORB” axial magmatism in the  
767 Oman ophiolite: The evidence against a mid-ocean ridge origin. *Geology* 41, 459-462,  
768 doi:410.1130/G33904.33901.
- 769 McNamara, A.K., Zhong, S., 2005. Thermochemical structures beneath Africa and the Pacific  
770 Ocean. *Nature* 437, 1136–1139.
- 771 Marzoli, A., Renne, P.R., Piccirillo, E.M., Ernesto, M., Bellieni, M.G., De Min, A., 1999.  
772 Extensive 200-million-year-old continental flood basalts of the central Atlantic  
773 magmatic province. *Science* 284, 616–618.
- 774 Matte, P., 2001. The Variscan collage and orogeny (480±290 Ma) and the tectonic definition  
775 of the Armorica microplate: a review. *Terra Nova* 13.
- 776 McHargue, T.R., Heidrick, T.L., Livingston, J.E., 1992. Tectonostratigraphic development of  
777 the Interior Sudan Rifts, Central Africa. *Tectonophysics* 213, 187-202.

- 778 McQuarrie, N., Stock, J.M., Verdel, C., Wernicke, B.P., 2003. Cenozoic evolution of  
779 Neotethys and implications for the causes of plate motions. *Geophys Res. Lett.* 30,  
780 2036, doi:10.1029/2003GL017992.
- 781 Menant, A., Jolivet, L., Vrielynck, B., 2015. From crustal to mantle dynamics, insight from  
782 kinematic reconstructions and magmatic evolution of the eastern Mediterranean region  
783 since the late Cretaceous. *Tectonophysics* submitted.
- 784 Milesi, J.P., Frizon de Lamotte, D., de Kock, G., Toteu, F., 2010. Tectonic Map of Africa,  
785 1:10 000 000 scale. CCGM-CGMW, Paris.
- 786 Monié, P., Agard, P., 2009. Coeval blueschist exhumation along thousands of kilometers:  
787 Implications for subduction channel processes. *Geochem. Geophys. Geosyst* 10,  
788 Q07002, doi:10.1029/2009GC002428.
- 789 Moucha, R., Forte, A.M., 2011. Changes in African topography driven by mantle convection.  
790 *Nature Geoscience* 4, 707-712, DOI: 10.1038/NGEO1235.
- 791 Mouthereau, F., Filleaudeau, P.Y., Vacherat, A., Pik, R., Lacombe, O., Fellin, M.G.,  
792 Castellort, S., Christophoul, F., Masini, E., 2014. Placing limits to shortening evolution  
793 in the Pyrenees: Role of margin architecture and implications for the Iberia/Europe  
794 convergence. *Tectonics* 33, 2283–2314, doi:10.1002/2014TC003663.
- 795 Mouthereau, F., Lacombe, O., Vergés, J., 2012. Building the Zagros collisional orogen:  
796 Timing, strain distribution and the dynamics of Arabia/Eurasia plate convergence.  
797 *Tectonophysics* 532-535, 27-60, doi:10.1016/j.tecto.2012.1001.1022.
- 798 Müller, R.D., Sdrolias, M., Gaina, C., Roest, W.R., 2008. Age, spreading rates, and spreading  
799 asymmetry of the world's ocean crust. *Geochem. Geophys. Geosyst* 9, Q04006,  
800 doi:10.1029/2007GC001743.
- 801 Müller, R.D., Sdrolias, M., Gaina, C., Steinberger, B., Heine, C., 2008. Long-term sea-level  
802 fluctuations driven by ocean basin dynamics. *Science* 319, 1357–1362.
- 803 Nicolas, A., 1989. Structures of ophiolites and dynamic of oceanic lithosphere. Kluwer Acad.  
804 Publ., Dordrecht.
- 805 Nikishin, A.M., Okay, A., Tüysüz, O., Demirer, A., Amelin, N., Petrov, E., 2015a. The Black  
806 Sea basins structure and history: New model based on new deep penetration regional  
807 seismic data. Part 1: Basins structure and fill. *Marine and Petroleum Geology* 59, 638-  
808 655, <http://dx.doi.org/610.1016/j.marpetgeo.2014.1008.1017>.
- 809 Nikishin, A.M., Okay, A., Tüysüz, O., Demirer, A., Wannier, M., Amelin, N., Petrov, E.,  
810 2015b. The Black Sea basins structure and history: New model based on new deep

- 811 penetration regional seismic data. Part 2: Tectonic history and paleogeography. *Marine*  
812 *Pet. Geology* 59, 656-670, [dx.doi.org/10.1016/j.marpetgeo.2014.1008.1018](https://doi.org/10.1016/j.marpetgeo.2014.1008.1018).
- 813 Nishikin, A.M., Cloething, S., Brunet, M.F., Stephenson, R.A., Bolotov, S.N., Ershov, A.V.,  
814 1998. Scythian platform, Caucasus and Black Sea region: Mesozoic- Cenozoic tectonic  
815 history and dynamics, in: Crasquin-Soleau, S., Barrier, E. (Eds.), *Peri-Tethys Memoir 3:*  
816 *stratigraphy and evolution of Teri-Tethyan platforms*, Paris, pp. 163-176.
- 817 Oberhänsli, R., Bousquet, R., Engi, M., Goffé, B., Gosso, G., Handy, M., Höck, V., Koller,  
818 F., Lardeaux, J.M., Polino, R., Rossi, P., Schuster, R., Schwartz, S., Spalla, I., 2004.  
819 *Metamorphic structure of the Alps*, edited by the Commission for the Geological Map  
820 of the World. *Mit. österr. geol. Ges.* 149.
- 821 Okay, A.I., 1989. Geology of the Menderes Massif and the Lycian Nappes south of Denizli,  
822 western Taurides. *Mineral Res. Expl. Bull.* 109, 37-51.
- 823 Okay, A., Tüysüz, O., 1999. Tethyan sutures of northern Turkey, in: Durand, B., Jolivet, L.,  
824 Horvath, F., Séranne, M. (Eds.), *The Mediterranean basins: Tertiary extension within*  
825 *the alpine orogen*. Geological Society, London, pp. 475-515.
- 826 Pearce, J.A., Alabaster, T., Shelton, A.W., Searle, M.P., 1981. The Oman ophiolite as a  
827 Cretaceous arc-basin complex: evidence and implications. *Phil. Transact. Roy. Soc.*  
828 300, 299-317.
- 829 Petters, S.W., 1983. Gulf of Guinea planktonic foraminiferal biochronology and geological  
830 history of the South Atlantic. *Journal of Foraminiferal Research* 13, 32-59.
- 831 Pourteau, A., Sudo, M., Candan, O., Lanari, P., Vidal, O., Oberhänsli, R., 2013.  Neotethys  
832 closure history of Anatolia: insights from  $^{40}\text{Ar}$ – $^{39}\text{Ar}$  geochronology and P–T  
833 estimation in high-pressure metasedimentary rocks. *J. metamorphic Geol.* 31, 585–606,  
834 [doi:10.1111/jmg.12034](https://doi.org/10.1111/jmg.12034).
- 835 Replumaz, A., Guillot, S., Villaseñor, A., Negredo, A.M., 2013. Amount of Asian  
836 lithospheric mantle subducted during the India/Asia collision. *Gondwana Research* 24,  
837 936-945, [http://dx.doi.org/10.1016/j.gr.2012.1007.1019](https://dx.doi.org/10.1016/j.gr.2012.1007.1019).
- 838 Ricard, Y., Richards, M.A., Lithgow-Bertelloni, C., LeStunff, Y., 1993. Geodynamic model  
839 of mantle density heterogeneity. *J. Geophys. Res.* 98, 21895–21909.
- 840 Ricou, L.E., 1971. Le croissant ophiolitique péri-arabe, une ceinture de nappes mise en place  
841 au crétacé supérieur. *Revue de géographie physique et de géologie dynamique* 13, 327-  
842 350.

- 843 Ricou, L.E., 1994. Tethys reconstructed: plates, continental fragments and their boundaries  
844 since 260 Ma from Central America to south-eastern Asia. *Geodinamica Acta* 7, 169-  
845 218.
- 846 Riley, T.R., Millar, I.L., Watkeys, M.K., Curtis, M.L., Leat, P.T., Klausen, M.B., Fanning,  
847 C.M., 2004. U-Pb zircon (SHRIMP) ages for the Lebombo rhyolites, South Africa:  
848 Refining the duration of Karoo volcanism. *J. Geol. Soc. London* 161, 547–550.
- 849 Rioux, M., Bowring, S., Kelemen, P., Gordon, S., Miller, R., Dudás, F., 2013. Tectonic  
850 development of the Samail ophiolite: High-precision U-Pb zircon geochronology and  
851 Sm-Nd isotopic constraints on crustal growth and emplacement. *J. Geophys. Res.* 118,  
852 1-17, doi:10.1002/jgrb.50139.
- 853 Ritsema, H.J., van Heijst, J.H., Woodhouse, J.H., 1999. Complex shear velocity structure  
854 beneath Africa and Iceland. *Science* 286, 1925–1928.
- 855 Rolland, Y., Billo, S., Corsini, M., Sosson, M., Galoyan, G., 2009. Blueschists of the  
856 Amassia-Stepanavan Suture Zone (Armenia): linking Tethys subduction history from E-  
857 Turkey to W-Iran. *Int J Earth Sci (Geol Rundsch)* 98, 533-550, DOI 10.1007/s00531-  
858 00007-00286-00538.
- 859 Rosenbaum, G., Lister, G.S., Duboz, C., 2002. Relative motions of Africa, Iberia and Europe  
860 during Alpine orogeny. *Tectonophysics* 359, 117–129.
- 861 Rossetti, F., Nasrabad, M., Theye, T., Gerdes, A., Monié, P., Lucci, F., Vignaroli, G., 2014.  
862 Adakite differentiation and emplacement in a subduction channel: The late Paleocene  
863 Sabzevar magmatism (NE Iran). *Geol. Soc. Am. Bull.*, doi:10.1130/B30913.30911.
- 864 Rossetti, F., Nasrabad, M., Vignaroli, G., Theye, T., Gerdes, A., Razavi, M.H., Vaziri, H.M.,  
865 2010. Early Cretaceous migmatitic mafic granulites from the Sabzevar range (NE Iran):  
866 implications for the closure of the Mesozoic peri-Tethyan oceans in central Iran. *Terra*  
867 *Nova* 22, 26-34, doi: 10.1111/j.1365-3121.2009.00912.x.
- 868 Schmid, S.M., Bernoulli, D., Fügenschuh, B., Matenco, L., Schefer, S., Schuster, R., Tischler,  
869 M., Ustaszewski, K., 2008. The Alpine-Carpathian-Dinaridic orogenic system:  
870 correlation and evolution of tectonic units. *Swiss J. Geosci.* 101, 139–183, DOI  
871 10.1007/s00015-00008-01247-00013.
- 872 Searle, M.P., Warren, C.J., Waters, D.J., Parrish, R.R., 2004. Structural evolution,  
873 metamorphism and restoration of the Arabian continental margin, Saih Hatat region,  
874 Oman mountains. *J. Struct. Geol.* 26, 451-473.



- 875 Searle, M.P., Waters, D.J., Martin, H.N., rex, D.C., 1994. Structure and metamorphism of  
876 blueschist-eclogite facies rocks from the northeastern Oman Mountains. *J. Struct. Geol.*  
877 151, 555-576.
- 878 Şengör, A.M.C., Burke, K., 1978. Relative timing of rifting and volcanism on Earth and its  
879 tectonic implications. *Geophys. Res. Lett.* 5, 419–421,  
880 doi:410.1029/GL1005i1006p00419.
- 881 Sengör, A.M.C., Stock, J., 2014. The Ayyubid Orogen: an ophiolite obduction-driven orogen  
882 in the late Cretaceous on the Neo-Tethyan south margin. *Geoscience Canada* 41, 225-  
883 254, dx.doi.org/210.12789/geocanj.12014.12741.12042.
- 884 Sengör, A.M.C., Yilmaz, Y., 1981. Tethyan evolution of Turkey: a plate tectonic approach.  
885 *Tectonophysics* 75, 181-241.
- 886 Stampfli, G.M., Borel, G.D., 2002. A plate tectonic model for the Paleozoic and Mesozoic  
887 constrained by dynamic plate boundaries and restored synthetic oceanic isochrons.  
888 *Earth Planet. Sci. Lett.* 196, 17-33.
- 889 Steinberger, B., 2000. Slabs in the lower mantle—Results of dynamic modeling compared  
890 with tomographic images and the geoid. *Phys. Earth Planet. Inter.* 118, 241–257.
- 891 Stoddard, P.R., Abbott, D., 1996. Influence of the tectosphere upon plate motion. *J. Geophys.*  
892 *Res.* 101, 5425-5433.
- 893 Svensen, H., Corfu, F., Polteau, S., Hammer, O., Planke, S., 2012. Rapid magma  
894 emplacement in the Karoo Large Igneous Province. *Earth Planet. Sci. Lett.* 325-326,  
895 1-9, doi:10.1016/j.epsl.2012.1001.1015.
- 896 Swezey, C.S., 2009. Cenozoic stratigraphy of the Sahara, Northern Africa. *Journal of African*  
897 *Earth Sciences* 53, 89-121, doi:110.1016/j.jafrearsci.2008.1008.1001.
- 898 Torsvik, T.H., Burke, K., Steinberger, B., Webb, S.J., Ashwal, L.D., 2010. Diamonds  
899 sampled by plumes from the core–mantle boundary. *Nature* 466, 352-355;  
900 doi:310.1038/nature09216.
- 901 Torsvik, T.H., Smethurst, M.A., Burke, K., Steinberger, B., 2006. Large igneous provinces  
902 generated from the margins of the large low-velocity provinces in the deep mantle.  
903 *Geophys. J. Int.* 167, 1447–1460, doi: 1410.1111/j.1365-1246X.2006.03158.x.
- 904 Torsvik, T.H., van der Voo, R., Doubrovine, P.V., Burke, K., Steinberger, B., Ashwal, L.D.,  
905 Trønnes, R.G., Webb, S.J., Bull, A.L., 2014. Deep mantle structure as a reference frame  
906 for movements in and on the Earth. *PNAS* 111, 8735-8740,  
907 www.pnas.org/cgi/doi/8710.1073/pnas.1318135111.



- 908 Turner, S., Regelous, M., Kelley, S., Hawkesworth, C., Mantovani, M., 1994. Magmatism  
909 and continental break-up in the South Atlantic: high precision  $^{40}\text{Ar}$ - $^{39}\text{Ar}$   
910 geochronology. *Earth Planet. Sci. Lett.* 121, 333-348.
- 911 van der Meer, D.G., Spakman, W., van Hinsbergen, D.J.J., Amaru, M.L., Torsvik, T.H., 2010.  
912 Towards absolute plate motions constrained by lower-mantle slab remnants. *Nature*  
913 *Geoscience* 3, 36-39; DOI: 10.1038/NGEO1708.
- 914 Van der Voo, R., Spakman, W., Bijwaard, H., 1999. Tethyan subducted slabs under India.  
915 *Earth Planet. Sci. Lett.* 171, 7-20.
- 916 van Hinsbergen, D.J.J., Steinberger, B., Doubrovine, P.V., Gassmüller, R., 2011. Acceleration  
917 and deceleration of India - Asia convergence since the Cretaceous: Roles of mantle  
918 plumes and continental collision. *J. Geophys. Res.* 116, B06101,  
919 doi:06110.01029/02010JB008051.
- 920 Vaughan, A.P.M., Scarrow, J.H., 2003. Ophiolite obduction pulses as a proxy indicator of  
921 superplume events? *Earth and Planetary Science Letters* 213, 407-416,  
922 doi:10.1016/S0012-1821X(1003)00330-00333.
- 923 Vergés, J., M Fernandez, Martinez, A., 2002. The Pyrenean orogen: pre-, syn-, and post-  
924 collisional evolution, in: Rosenbaum, G., Lister, G.S. (Eds.), *Reconstruction of the*  
925 *evolution of the Alpine-Himalayan orogen*, pp. 57-76.
- 926 Vergés, J., Sabat, F., 1999. Constraints on the western Mediterranean kinematic evolution  
927 along a 1000 km transect, from Iberia to Africa, in: Durand, B., Jolivet, L., Horvath, F.,  
928 Séranne, M. (Eds.), *The Mediterranean basins: Tertiary extension within the Alpine*  
929 *orogen*. Geological Society, London, pp. 63-80.
- 930 Wenekers, J.H.N., Wallace, F.K., Abugares, Y.I., 1996. The geology and hydrocarbons of  
931 the Sirt Basin: a synopsis, in: Salem, M.J., Mouzoughi, A.J., Hammuda, O.S. (Eds.), *The*  
932 *geology of Sirt Basin*. Elsevier, Amsterdam, pp. 3-55.
- 933 Wilson, M., 1993. Magmatism and the geodynamics of basin formation. *Sedimentary*  
934 *Geology* 86, 5-29.
- 935 Wilson, M., Guiraud, R., 1992. Magmatism and rifting in Western and Central Africa, from  
936 Late Jurassic to Recent times. *Tectonophysics* 213, 203-225.
- 937 Yamato, P., Agard, P., Goffé, B., De Andrade, V., Vidal, O., Jolivet, L., 2007. New, high  
938 precision P-T estimates for Oman blueschists: implications for obduction, nappe  
939 stacking and exhumation processes. *J. Metamorphic Geol.* 25, 657-682.
- 940 Zahirovic, S., Müller, R.D., Seton, M., Flament, N., 2015. Tectonic speed limits from plate  
941 kinematic reconstructions. *Earth Planet. Sci. Lett.* 418, 40-52,

942 <http://dx.doi.org/10.1016/j.epsl.2015.1002.1037>.

943 Ziegler, P.A., 1992. Plate tectonics, plate moving mechanisms and rifting. *Tectonophysics*,  
944 215, 9-34.

945

946

Draft

947 **Figure caption**

948

949

950 Figure 1: reconstructions of Africa and the Tethys Ocean from the Late Jurassic to the  
951 Present. Plate kinematics is based upon Barrier and Vrielynck (2008), Jolivet et al. (2003) and  
952 Menant et al. (2015). Thick grey lines represent the motion paths of three points of Africa  
953 across the reconstructions. The detailed paths with the successive points are shown on figure  
954 1H (Present stage) with ages in Ma. Thick blue lines along the paths represent the average  
955 direction of motion at the time of reconstruction. Further explanation in text.

956

957 Figure 2: Compilation of indicators of mantle convection activity and tectonic and  
958 metamorphic events related with the Late Cretaceous compression and obduction event.  
959 Green shadings represent the periods of faster Africa-Eurasia convergence, faster spreading in  
960 the South Atlantic and compressional period in Africa in the Late Cretaceous. 1-6: Spreading  
961 rates after Conrad and Lithgow-Bertelloni (2007) and Colli et al. (2014). 1: West Indian  
962 Ridge. 2: South Atlantic Ridge. 2b: South Atlantic full spreading rate. 3: West Pacific. 4: East  
963 Pacific. 5: Global average. 6: Global average with Farallon. Most of the average value  
964 originates in the Pacific ridges, especially the peak around 120-110 Ma. Although velocities  
965 are much lower, the South Atlantic ridge shows an increased velocity between 120 and 70  
966 Ma. 7-8: Global figure of formation of oceanic crust and sea level variations. The Pacific peak  
967 of accretion in the Pacific reflects on the global production rates and the first order high in the  
968 sea level is coeval with this globally high production rates in the Cretaceous. 7: Sea-level after  
969 Müller et al. (2008). 8: Global oceanic flux (ridges and plateaus) after Cogné and Humler  
970 (2006). 9: LIPS after Gaina et al. (2013) Mad. Agh: Madagascar-Agulhas, SWI: South West  
971 Indian, SEA: South East Atlantic. 10-14: African plate velocity. All models of the Africa-  
972 Eurasia convergence show an increase between 120 Ma and 70 Ma that is coeval with the  
973 higher velocity along the South Atlantic Ridge. Absolute velocity models show different  
974 figures and the peak of velocity is either between 110 and 100 Ma or around 80-70 Ma. 10:  
975 Africa-Eurasia convergence velocity at the longitude of the West Mediterranean after  
976 Rosenbaum et al. (2002). 11: Africa absolute velocity (Dobrovine et al. 2012; Gaina et al.  
977 2013) based on moving hot spots and a true polar wander model before 124 Ma. 12: Africa  
978 RMS velocity, hybrid moving hotspots and true polar wander corrected reference frame  
979 (Zahirovic et al. 2015). 13: Africa/Eurasia convergence velocity at the longitude of Oman  
980 (Agard et al. 2007). 14-15: India plate velocity. The velocity peak is recorded after the peak

981 for Africa, around 60 Ma. 14: India absolute velocity (van Hinsbergen et al. 2011). 15:  
982 India/Asia convergence (van Hinsbergen et al. 2011). 16: Sediments accumulation rates on  
983 South African margins (Guillocheau et al. 2012). The peak centered on 80 Ma comes after a  
984 period of increasing sediment discharge and a period of uplift and erosion of South Africa. 17:  
985 Subsidence of Northern Africa (Guiraud et al. 2005). 18: Timing of subduction, exhumation  
986 and back-arc extension in the Western Mediterranean (Jolivet et al. 2003). 19: Timing of  
987 subduction, exhumation and back-arc extension in the Western Mediterranean (Jolivet and  
988 Brun 2010; Jolivet et al. 2003). 20: folding in the Paris Basin (Guillocheau et al. 2000). 21:  
989 Timing of subduction and obduction in Oman (Agard et al. 2007; Hacker et al. 1996; Nicolas  
990 1989; Rioux et al. 2013). 22: Timing of subduction and obduction in Turkey (Celik et al.  
991 2011; Pourteau et al. 2013). 23: Timing of subduction and obduction in Armenia (Hässig et  
992 al. 2015; Hässig et al. 2013; Rolland et al. 2009). 24: Timing of subduction and obduction in  
993 the Zagros Internal Zones (Agard et al. 2006; 2005; 2011). 25: Timing of subduction and  
994 obduction in the Sabzevar Zone in Iran (Rossetti et al. 2014; 2010). 26: Timing of subduction  
995 and obduction in Sistan (Iran) (Angiboust et al. 2013; Monié and Agard 2009). 27: Tectonic  
996 timing in the Black Sea region (Hippolyte et al. 2010; Nikishin et al. 2015a; Nikishin et  
997 al., 2015b). 28: Tectonometamorphic timing in the Himalayas (Guillot and Replumaz 2013).

998  
999 Figure 3: Tectonic and volcanic features of Africa and the Mediterranean and lower mantle  
1000 seismic velocity anomalies (1000 km, SMEAN model (Becker and Boschi 2002)). Upper  
1001 panel: Tectonic map of Africa after Milesi et al. (2010) and the Mediterranean region showing  
1002 the main Cretaceous Rifts (in light green), and the main volcanic provinces (Afar in red, SW  
1003 Indian Ocean, Madagascar-Agulhas, Etendeka and CAMP in violet, Karoo in blue). Dark  
1004 green dots are the main kimberlites (Jelsma et al. 2004; 2009). Lower panel: SMEAN  
1005 tomographic model and the outline of the Neo-Tethys slab in the lower mantle after Faccenna  
1006 et al. (2013a).

1007

1008 Figure 4: Scenario linking the Late Cretaceous obduction of the Tethyan ophiolites on Apulia  
1009 and Africa to convection. A: ~170 Ma. An established conveyor belt with plume push and  
1010 slab pull below Africa drags continental blocks northward away from the main African plate,  
1011 forming the Apulia micro-continent. The whole system is under extension, rifts develop far  
1012 within the African plate (Late Jurassic –Early Cretaceous). B: ~90 Ma. The slab has detached  
1013 below Eurasia and the African plate is driven by plume push and less slab pull. The plume  
1014 beneath South of Africa is more active and accelerates the northward drift of Africa and

1015 pushes the African slab faster in the mantle thus rendering subduction more difficult and  
1016 putting the whole system under compression. Compression during penetration of the slab in  
1017 the lower mantle induces shortening within Africa and Eurasia and initiates a new subduction  
1018 along the northern margin of Africa, leading to obduction of the oceanic crust onto the  
1019 continental margin (100-90 Ma.). At maximum compression shortening propagates far inside  
1020 Africa reactivating all the Cretaceous rifts (Santonian event, 85 Ma). C: 80-70 Ma. Slab  
1021 avalanches in the lower mantle and a progressive relaxation of compressional stresses ensues.  
1022 D: ~30 Ma. After full penetration, the conveyor belt is functional again. The slab is deep into  
1023 the lower mantle like below the Aegean and retreats. Back-arc extension in the upper plate is  
1024 observed. Extension is active above the northward moving plume leading to the separation of  
1025 Arabia from the main body of the African plate.

1026

1027 Figure 5: a scenario of obduction driven by basal drag. Northward movement of the  
1028 asthenospheric mantle with respect to Africa favours the subduction of the sub-continental  
1029 lithospheric mantle below the young and light oceanic one.

1030

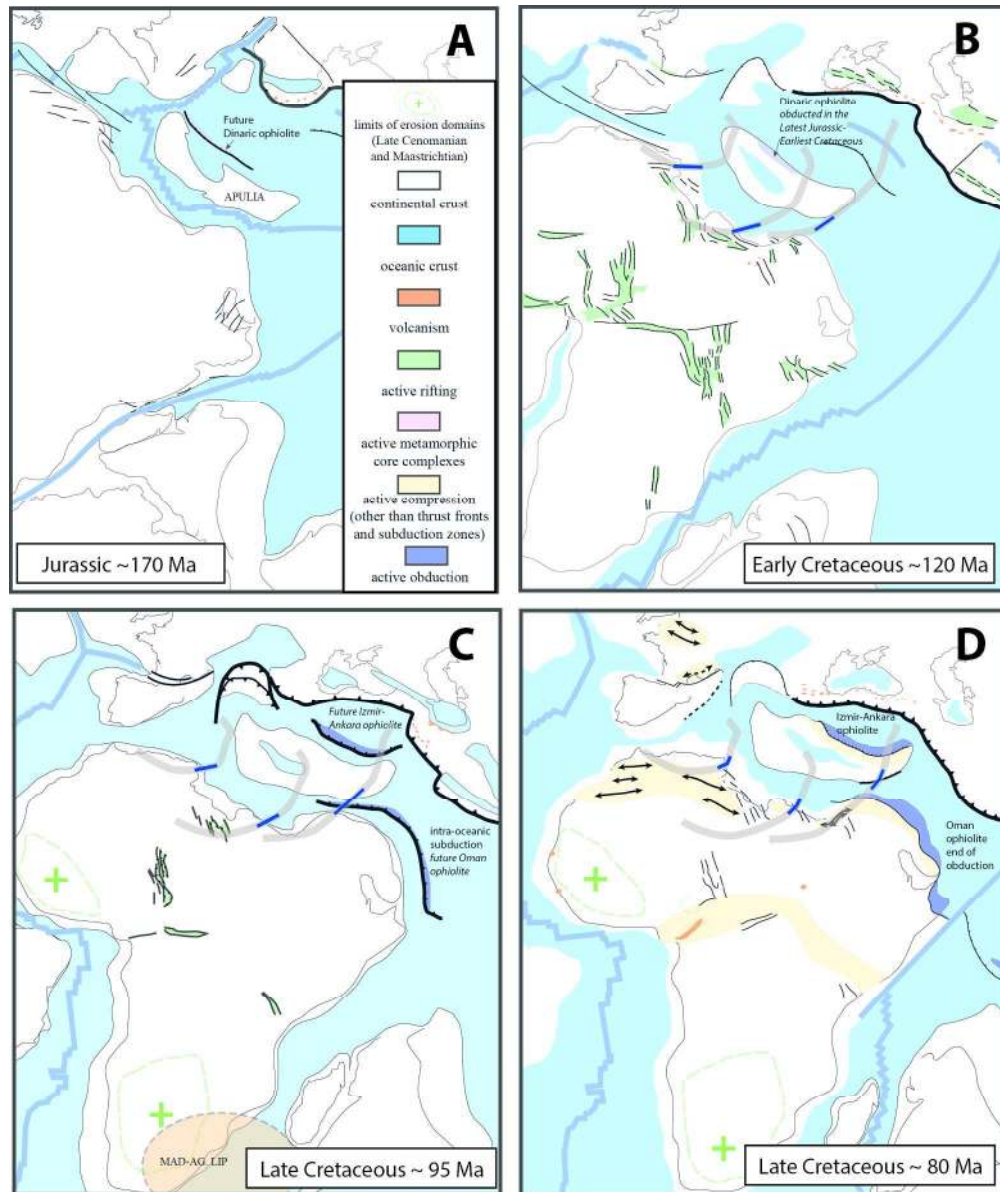


Figure 1: reconstructions of Africa and the Tethys Ocean from the Late Jurassic to the Present. Plate kinematics is based upon Barrier and Vrielynck (2008), Jolivet et al. (2003) and Menant et al. (2015). Thick grey lines represent the motion paths of three points of Africa across the reconstructions. The detailed paths with the successive points are shown on figure 1H (Present stage) with ages in Ma. Thick blue lines along the paths represent the average direction of motion at the time of reconstruction. Further explanation in text.

192x229mm (300 x 300 DPI)



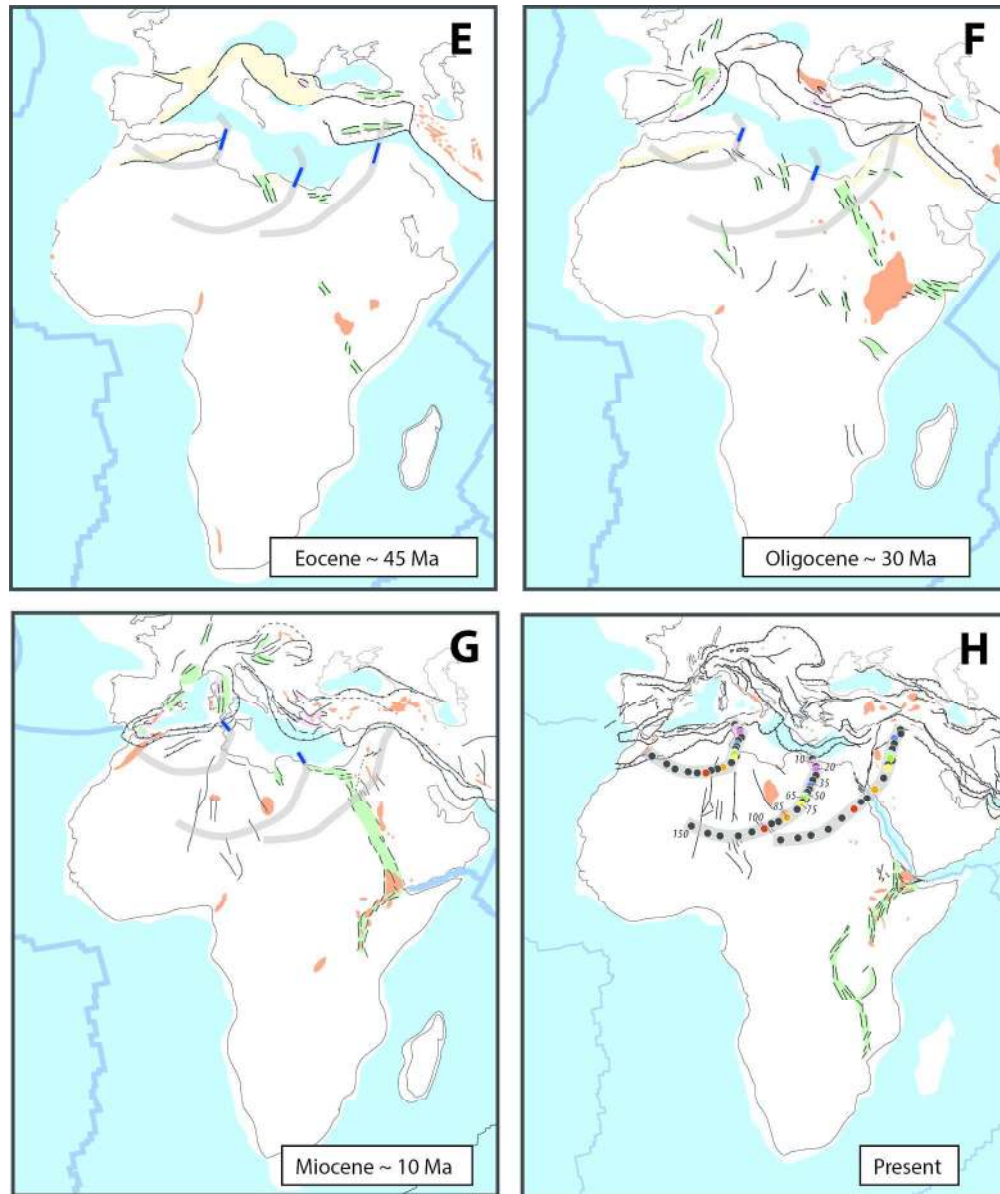


Figure 1: reconstructions of Africa and the Tethys Ocean from the Late Jurassic to the Present. Plate kinematics is based upon Barrier and Vrielynck (2008), Jolivet et al. (2003) and Menant et al. (2015). Thick grey lines represent the motion paths of three points of Africa across the reconstructions. The detailed paths with the successive points are shown on figure 1H (Present stage) with ages in Ma. Thick blue lines along the paths represent the average direction of motion at the time of reconstruction. Further explanation in text.

193x230mm (300 x 300 DPI)



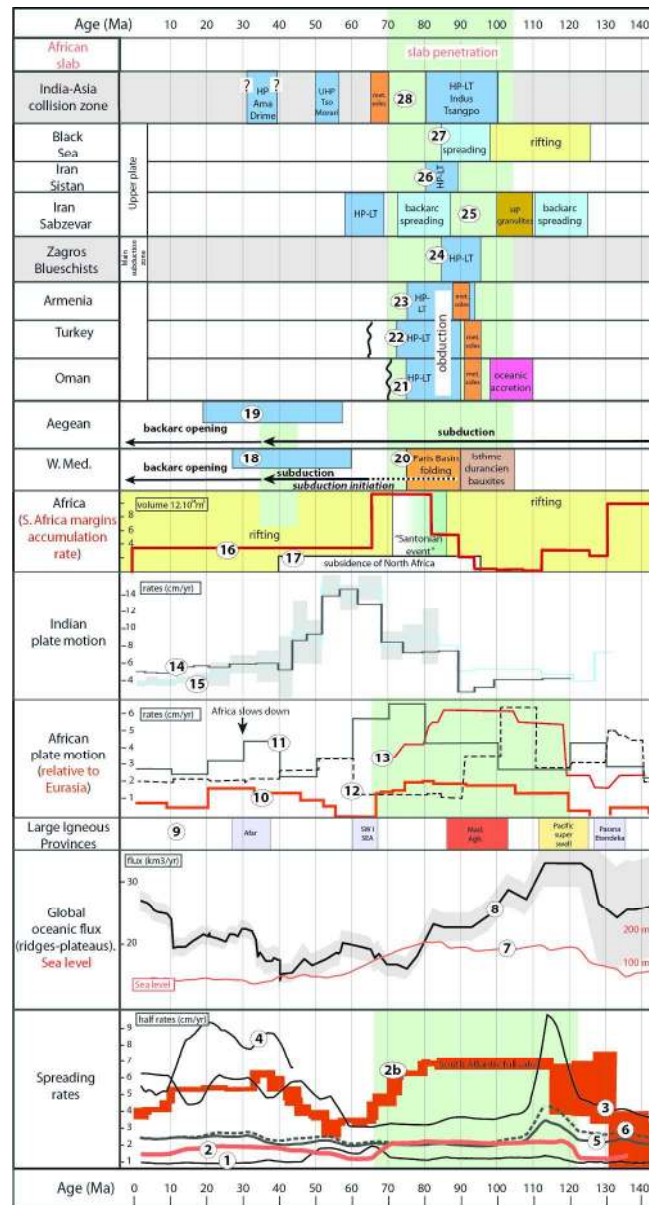


Figure 2: Compilation of indicators of mantle convection activity and tectonic and metamorphic events related with the Late Cretaceous compression and obduction event. Green shadings represent the periods of faster Africa-Eurasia convergence, faster spreading in the South Atlantic and compressional period in Africa in the Late Cretaceous. 1-6: Spreading rates after Conrad and Lithgow-Bertelloni (2007) and Colli et al. (2014). 1: West Indian Ridge. 2: South Atlantic Ridge. 2b: South Atlantic full spreading rate. 3: West Pacific. 4: East Pacific. 5: Global average. 6: Global average with Farallon. Most of the average value originates in the Pacific ridges, especially the peak around 120-110 Ma. Although velocities are much lower, the South Atlantic ridge shows an increased velocity between 120 and 70 Ma. 7-8: Global figure of formation of oceanic crust and sea level variations. The Pacific peak of accretion in the Pacific reflects on the global production rates and the first order high in the sea level is coeval with this globally high production rates in the Cretaceous. 7: Sea-level after Müller et al. (Müller et al., 2008). 8: Global oceanic flux (ridges and plateaus) after Cogné and Humler (Cogné and Humler, 2006). 9: LIPS after Gaina et al. (Gaina et al., 2013) Mad. Agh: Madagascar-Agulhas, SWI: South West Indian, SEA: South East Atlantic. 10-14: African plate

velocity. All models of the Africa-Eurasia convergence show an increase between 120 Ma and 70 Ma that is coeval with the higher velocity along the South Atlantic Ridge. Absolute velocity models show different figures and the peak of velocity is either between 110 and 100 Ma or around 80-70 Ma. 10: Africa-Eurasia convergence velocity at the longitude of the West Mediterranean after Rosenbaum et al. (2002). 11: Africa absolute velocity (Dobrovine et al., 2012; Gaina et al., 2013) based on moving hot spots and a true polar wander model before 124 Ma. 12: Africa RMS velocity, hybrid moving hotspots and true polar wander corrected reference frame (Zahirovic et al., 2015). 13: Africa/Eurasia convergence velocity at the longitude of Oman (Agard et al., 2007). 14-15: India plate velocity. The velocity peak is recorded after the peak for Africa, around 60 Ma. 14: India absolute velocity (van Hinsbergen et al., 2011). 15: India/Asia convergence (van Hinsbergen et al., 2011). 16: Sediments accumulation rates on South African margins (Guillocheau et al., 2012). The peak centered on 80 Ma comes after a period of increasing sediment discharge and a period of uplift and erosion of South Africa. 17: Subsidence of Northern Africa (Guiraud et al., 2005). 18: Timing of subduction, exhumation and back-arc extension in the Western Mediterranean (Jolivet et al., 2003). 19: Timing of subduction, exhumation and back-arc extension in the Western Mediterranean (Jolivet and Brun, 2010; Jolivet et al., 2003). 20: folding in the Paris Basin (Guillocheau et al., 2000). 21: Timing of subduction and obduction in Oman (Agard et al., 2007; Hacker et al., 1996; Nicolas, 1989; Rioux et al., 139x243mm (300 x 300 DPI)

Draft

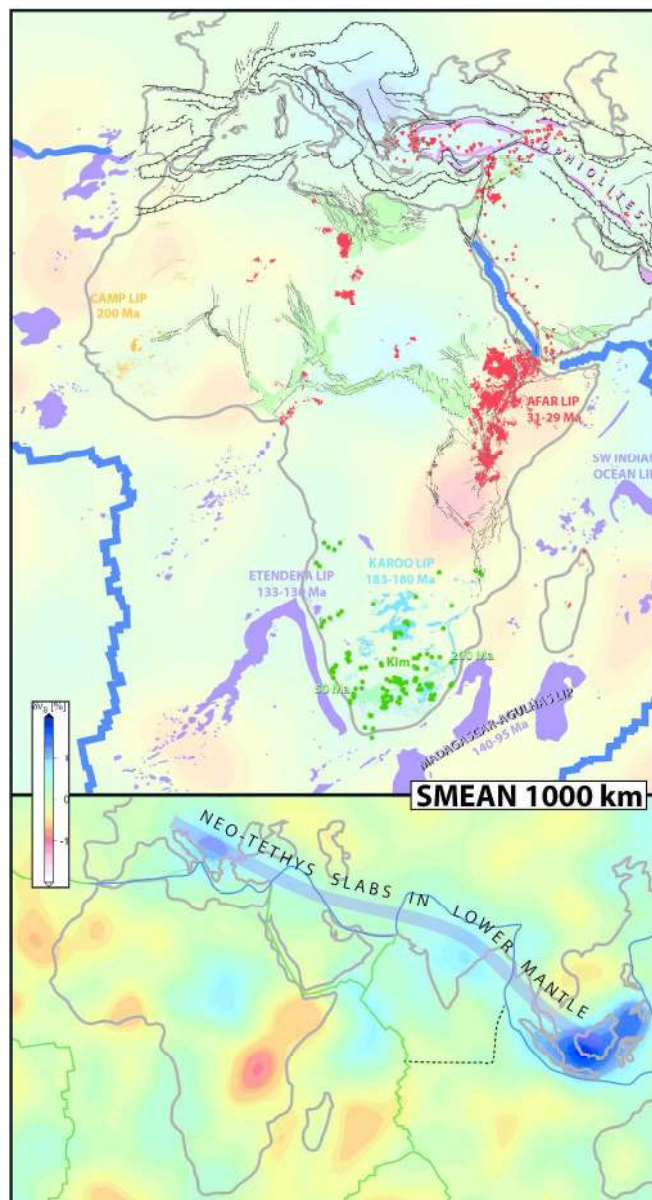


Figure 3: Tectonic and volcanic features of Africa and the Mediterranean and lower mantle seismic velocity anomalies (1000 km, SMEAN model (Becker and Boschi, 2002)). Upper panel: Tectonic map of Africa after Milesi et al. (2010) and the Mediterranean region showing the main Cretaceous Rifts (in light green), and the main volcanic provinces (Afar in red, SW Indian Ocean, Madagascar-Agulhas, Etendeka and CAMP in violet, Karoo in blue). Dark green dots are the main kimberlites (Jelsma et al., 2004; 2009). Lower panel: SMEAN tomographic model and the outline of the Neo-Tethys slab in the lower mantle after Faccenna et al. (2013a).

156x285mm (300 x 300 DPI)

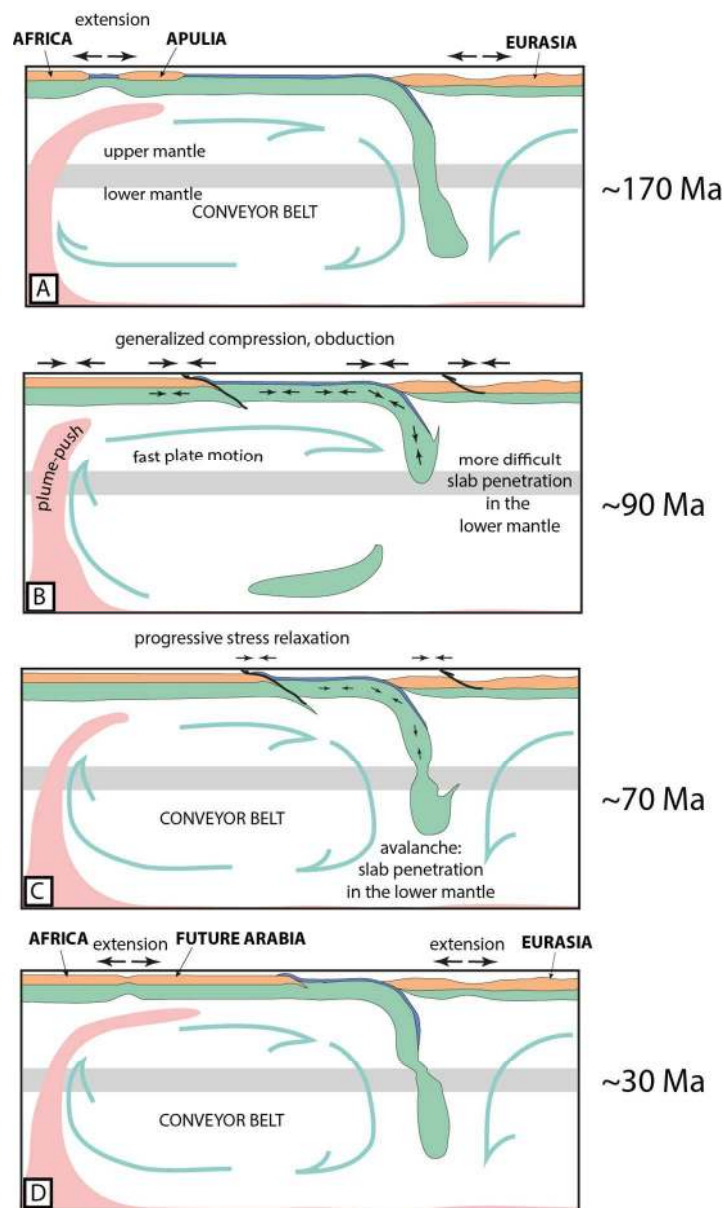


Figure 4: Scenario linking the Late Cretaceous obduction of the Tethyan ophiolites on Apulia and Africa to convection. A: ~170 Ma. An established conveyor belt with plume push and slab pull below Africa drags continental blocks northward away from the main African plate, forming the Apulia micro-continent. The whole system is under extension, rifts develop far within the African plate (Late Jurassic –Early Cretaceous). B: ~90 Ma. The slab has detached below Eurasia and the African plate is driven by plume push and less slab pull. The plume beneath South of Africa is more active and accelerates the northward drift of Africa and pushes the African slab faster in the mantle thus rendering subduction more difficult and putting the whole system under compression. Compression during penetration of the slab in the lower mantle induces shortening within Africa and Eurasia and initiates a new subduction along the northern margin of Africa, leading to obduction of the oceanic crust onto the continental margin (100-90 Ma.). At maximum compression shortening propagates far inside Africa reactivating all the Cretaceous rifts (Santonian event, 85 Ma). C: 80-70 Ma. Slab avalanches in the lower mantle and a progressive relaxation of compressional stresses ensues. D: ~30 Ma. After full penetration, the conveyor belt is functional again. The slab is deep

into the lower mantle like below the Aegean and retreats. Back-arc extension in the upper plate is observed. Extension is active above the northward moving plume leading to the separation of Arabia from the main body of the African plate.  
97x164mm (300 x 300 DPI)

Draft

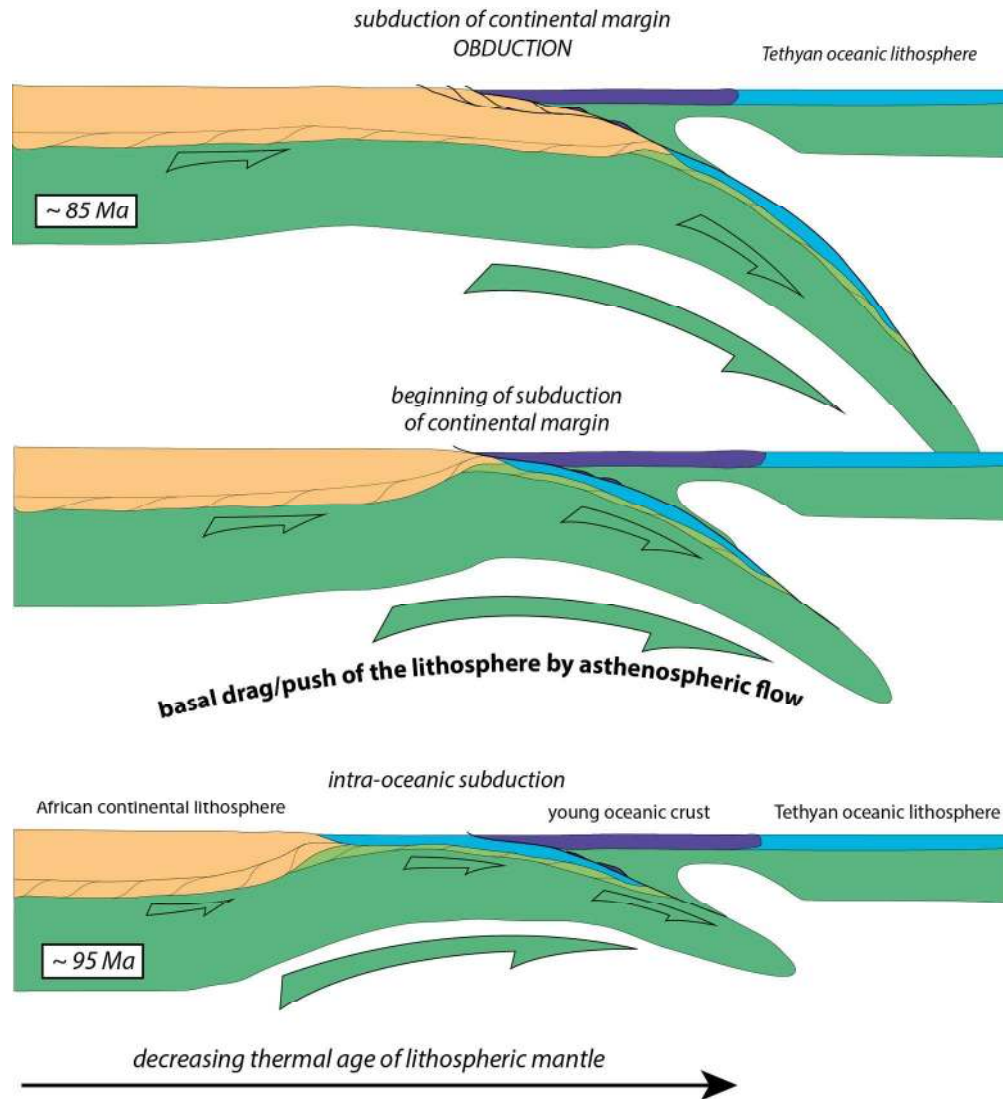


Figure 5: a scenario of obduction driven by basal drag. Northward movement of the asthenospheric mantle with respect to Africa favours the subduction of the sub-continental lithospheric mantle below the young and light oceanic one.

164x179mm (300 x 300 DPI)